Enhancing the effectiveness of Stirling engine regenerators

by

Anders S. Nielsen

A thesis submitted to the
School of Graduate and Postdoctoral Studies in partial
fulfillment of the requirements for the degree of

Master of Applied Science in Mechanical Engineering

The Faculty of Engineering and Applied Science

University of Ontario Institute of Technology

Oshawa, Ontario, Canada

April 2019

© Anders S. Nielsen, 2019

Thesis Examination Information

Submitted by: **Anders S. Nielsen**

Master of Applied Science in **Mechanical Engineering**

Thesis title: Enhancing the effectiveness of Stirling engine regenerators

An oral defense of this thesis took place on April 8th, 2019 in front of the following examining committee:

Examining Committee:

Chair of Examining Committee	Dr. Haoxiang Lang
Research Supervisor	Dr. Brendan MacDonald
Examining Committee Member	Dr. Dipal Patel
External Examiner	Dr. Bale Reddy, UOIT-FEAS

The above committee determined that the thesis is acceptable in form and content and that a satisfactory knowledge of the field covered by the thesis was demonstrated by the candidate during an oral examination. A signed copy of the Certificate of Approval is available from the School of Graduate and Postdoctoral Studies.

Abstract

A discrete heat transfer model is developed to determine which parameters influence the effectiveness of Stirling engine regenerators and quantify how they influence it. It is revealed that the regenerator thermal mass ratio and number of sub-regenerators are the two parameters that influence regenerator effectiveness, and these findings were extended to derive expressions for the regenerator effectiveness and Stirling engine efficiency. It is determined that a minimum of 19 sub-regenerators are required to attain a regenerator effectiveness of 95%. Experiments validated the heat transfer model, and demonstrated that stacking sub-regenerators, such as wire meshes, provides sufficient thermal resistance to generate a temperature distribution throughout the regenerator. This is the first study to determine how Stirling engine designers can attain a desired value for the regenerator effectiveness, and/or a desired value for the Stirling engine efficiency by selecting appropriate values of regenerator thermal mass ratio and number of sub-regenerators.

Keywords: Stirling engine; efficiency; regenerator; effectiveness; heat transfer

Author's Declaration

I hereby declare that this thesis consists of original work of which I have authored. This is a true copy of the thesis, including any required final revisions, as accepted by my examiners.

I authorize the University of Ontario Institute of Technology to lend this thesis to other institutions or individuals for the purpose of scholarly research. I further authorize the University of Ontario Institute of Technology to reproduce this thesis by photocopying or by other means, in total or in part, at the request of other institutions or individuals for the purpose of scholarly research. I understand that my thesis will be made electronically available to the public.

Anders Nielsen

Statement of Contributions

The work described in Chapter 2, 3, and 4 in this thesis have been submitted for publication as:

Anders S. Nielsen, Brayden T. York, and Brendan D. MacDonald (2019). Stirling engine regenerators: How to attain over 95% effectiveness. [Manuscript submitted for publication.]

I performed the literature review, numerical simulations, and derivations for the above manuscript, and also oversaw the experiments and presented the findings.

Brayden T. York, an undergraduate student at the University of Ontario Institute of Technology, designed and constructed the experimental apparatus described in Chapter 3, and performed the experiments.

Acknowledgements

I will begin by thanking the people who have played an influential role in my life during this rigorous and enlightening process.

I will first thank my supervisor, Dr. Brendan MacDonald, for his continuous encouragement, trust, and enthusiasm for the past four years, ever since I was a second year undergrad. In my time working under the supervision of Dr. Brendan MacDonald, I have learned more than I could ever have anticipated, and I can honestly say that I had fun. Thank you for everything. I will also thank my current and former lab mates: Md. Almostasim Mahmud, Noosheen Walji, Mosfera Chowdury, Soma Chakraborty, Salvatore Ranieri, Henry Fung, Michael Crowley, William Oishi, and Justin Rizzi for always being welcoming and making the workload seem bearable. Thank you to my supervisory committee, Dr. Dipal Patel and Dr. Brendan MacDonald, for dedicating their time to assess my work, and thank you to Dr. Bale Reddy for agreeing to be the external examiner and for thoroughly examining my work.

Penultimately, I will thank the love of my life, Nicole Krysa, for helping and supporting me throughout the entirety of my degree. You help me more than you know. Words cannot describe how appreciative I am of you.

Finally, I will thank my family, Carl, Barbara, and Chloe, for their unconditional love, and for shaping me into the person I am today. I would be nowhere without them.

Contents

List of Figures

Nomenclature

Symbols

Δt	time step (s)
ΔT_{reg}	temperature change caused by regenerator (K)
Nu	Nusselt number (-)
Pr	Prandtl number (-)
Pr_{avg}	average Prandtl number (-)
Re	Reynolds number (-)
A	regenerator surface area (m^2)
b	Nusselt number correlation exponent (-)
C_1	first correction coefficient (-)
C_2	second correction coefficient (-)
c_r	specific heat capacity of regenerator material (J/kg K)
$c_{v,f}$	constant volume specific heat capacity of working fluid (J/kg K)
D	regenerator wire diameter (m)
h	heat transfer coefficient (W/m^2 K)
k_f	thermal conductivity of working fluid (W/m K)
k_r	thermal conductivity of regenerator (W/m K)
m_f	mass of working fluid (kg)
m_r	mass of regenerator (kg)
N	number of sub-regenerators (-)

n	number of regenerator passes (-)
P_{max}	maximum pressure in Stirling cycle (Pa)
P_{min}	minimum pressure in Stirling cycle (Pa)
Q_{in}	heat added (J)
$Q_{non\text{-}reg}$	heat not transferred by working fluid (J)
Q_{out}	heat rejected (J)
R	working fluid ideal gas constant (J/kg K)
r	regenerator wire radius (m)
t	time (s)
T_f^p	working fluid temperature at current time step (K)
T_r^p	regenerator temperature at current time step (K)
$T_{sys,H}^{(1)}$	hot system settling temperature of first sub-regenerator (K)
$T_{sys,L}^{(1)}$	cold system settling temperature of first sub-regenerator (K)
$T_{sys,H}^{(i)}$	hot system settling temperature of inner sub-regenerators (K)
$T_{sys,L}^{(i)}$	cold system settling temperature of inner sub-regenerators (K)
$T_{sys,H}^{(N)}$	hot system settling temperature of last sub-regenerator (K)
$T_{sys,L}^{(N)}$	cold system settling temperature of last sub-regenerator (K)
T_f^{p+1}	working fluid temperature at successive time step (K)
T_r^{p+1}	regenerator temperature at successive time step (K)
T_f	working fluid temperature (K)
T_H	heat source temperature (K)
T_H/T_L	target temperature ratio (-)
T_L	heat sink temperature (K)
T_r	regenerator temperature (K)
$T_{f,final}$	final temperature of working fluid (K)
$T_{f,initial}$	initial temperature of working fluid (K)

$T_{r,final}$	final temperature of regenerator (K)
$T_{r,initial}$	initial temperature of regenerator (K)
t_{reg}	engine speed regeneration time (s)
$T_{sys,H}$	hot side system settling temperature (K)
$T_{sys,L}$	cold side system settling temperature (K)
T_{sys}	system settling temperature (K)
V	regenerator volume (m^3)
V_{max}	maximum volume of working fluid (m^3)
V_{min}	minimum volume of working fluid (m^3)

Greek Letters

$\epsilon_{reg,max}$	maximum regenerator effectiveness (-)
ϵ_{reg}	regenerator effectiveness (-)
η_{Carnot}	Carnot efficiency (-)
$\eta_{Stirling,ideal}$	ideal Stirling engine efficiency (-)
$\eta_{Stirling}$	Stirling engine efficiency (-)
γ	regenerator thermal mass ratio (-)
λ	compression ratio (-)
ω	Stirling engine rotational speed (rpm)
ρ	regenerator density (kg/m^3)
σ	standard deviation of sub-regenerator thermal mass ratio (-)
τ	time constant for regeneration (s)
ζ	regeneration time ratio (-)

Chapter 1

Introduction

1.1 Motivation

The development of feasible and sustainable energy technologies is critical due to increasing concerns surrounding greenhouse gas emissions and climate change. The vast majority of energy is generated by fossil fuel based systems, which contribute to 87% of the global demand, while hydro-electric and nuclear produce a combined 11%, and less than 2% is attributed to renewable energy sources [1]. Consequently, a staggering 35 billion tonnes of greenhouse gas is released into the atmosphere annually [1], which results in elevating global temperatures, and the increasing frequency and intensity of hurricanes in populated areas [2]. Hence, it is crucial that renewable technologies play a more prominent role in generating energy globally to mitigate society's dependence on fossil fuels, and to address the issues associated with climate change.

Solar and wind technologies have been developed to produce clean power from the

natural energy provided by the sun and wind, respectively, in an effort to relent climate change. However, wind and solar have unstable and intermittent power outputs due to the unreliable nature of their resources, making them unsuitable for small-scale applications that require on-demand power, including: remote communities, space equipment in unsheltered atmospheres, and hospital equipment after a natural disaster. For example, in the aftermath of a hurricane (Figure 1.1), a hospital's reserves of diesel fuel decrease rapidly to supply emergency power to medical equipment, requiring staff to prioritize the distribution of life-saving treatment. Additionally, replenishing the reserves of diesel fuel is virtually impossible since the transportation infrastructure has been devastated by the hurricane, eventually rendering the medi-

Figure 1.1: Memorial Medical Center in New Orleans in the aftermath of hurricane Katrina in 2005. Image courtesy of *The Guardian*. [3]

cal equipment useless. Solar technologies are unable to produce overnight power and negligible amounts on cloudy days, and wind technologies are incapable of producing power during calm periods, therefore making them unsuitable for the previous applications. Accordingly, the development of renewable technologies that have the ability to provide continuous power from a wide range of sustainable energy sources, and can offer versatility in emergency applications is desirable.

A promising technology that can be implemented to offer flexibility in emergency situations, and can also alleviate the global demand for clean energy is the Stirling engine. The Stirling engine is an external combustion engine, meaning that it has the ability to transfer thermal energy from an outside fuel source to the working fluid inside the engine to produce power. This feature enables Stirling engines to rely on sustainable energy sources, such as solar thermal, to eliminate greenhouse gas emissions; and in dire circumstances, fuel sources can include the debris left by the hurricane or diesel fuel to operate on demand. Essentially anything that can produce sufficient heat can be used as a fuel source to power the Stirling engine, thus promoting its versatility for a wide range of applications. Therefore, it is critical that the performance and efficiency of Stirling engines improve in order to enhance their ability to address the aforementioned demands.

1.2 Background

1.2.1 The Stirling cycle

The Stirling cycle consists of four thermodynamic processes: isothermal heat addition (1-2), isochoric regenerative cooling (2-3), isothermal heat rejection (3-4), and isochoric regenerative heating (4-1), which are shown in Figure 1.2(a). These processes enable the Stirling cycle to have the highest theoretical efficiency, which is known as the Carnot efficiency. The components of the Stirling engine that enable it to complete the Stirling cycle are the heater, cooler, hot piston, cold piston, working fluid, and regenerator, which are shown in Figure 1.2(b). The regenerator is often composed of multiple wire mesh sub-regenerators constructed from a material with a relatively high thermal conductivity and heat capacity, such as stainless steel or copper. The employed working fluid is typically hydrogen, helium, or air, and therefore the ideal gas law is used to determine the temperature and pressure of the working fluid at each stage of the Stirling cycle. The Stirling engine operates on a closed cycle, meaning that the mass of the working fluid in the engine remains constant throughout the entire cycle, and is not purged into the atmosphere or replenished with new fluid. The expansion and compression of the working fluid by the hot and cold pistons, coupled with the regenerative heating and cooling processes, enable the Stirling engine to produce power. Each of the Stirling engine's thermodynamic processes are described in detail in the following sections.

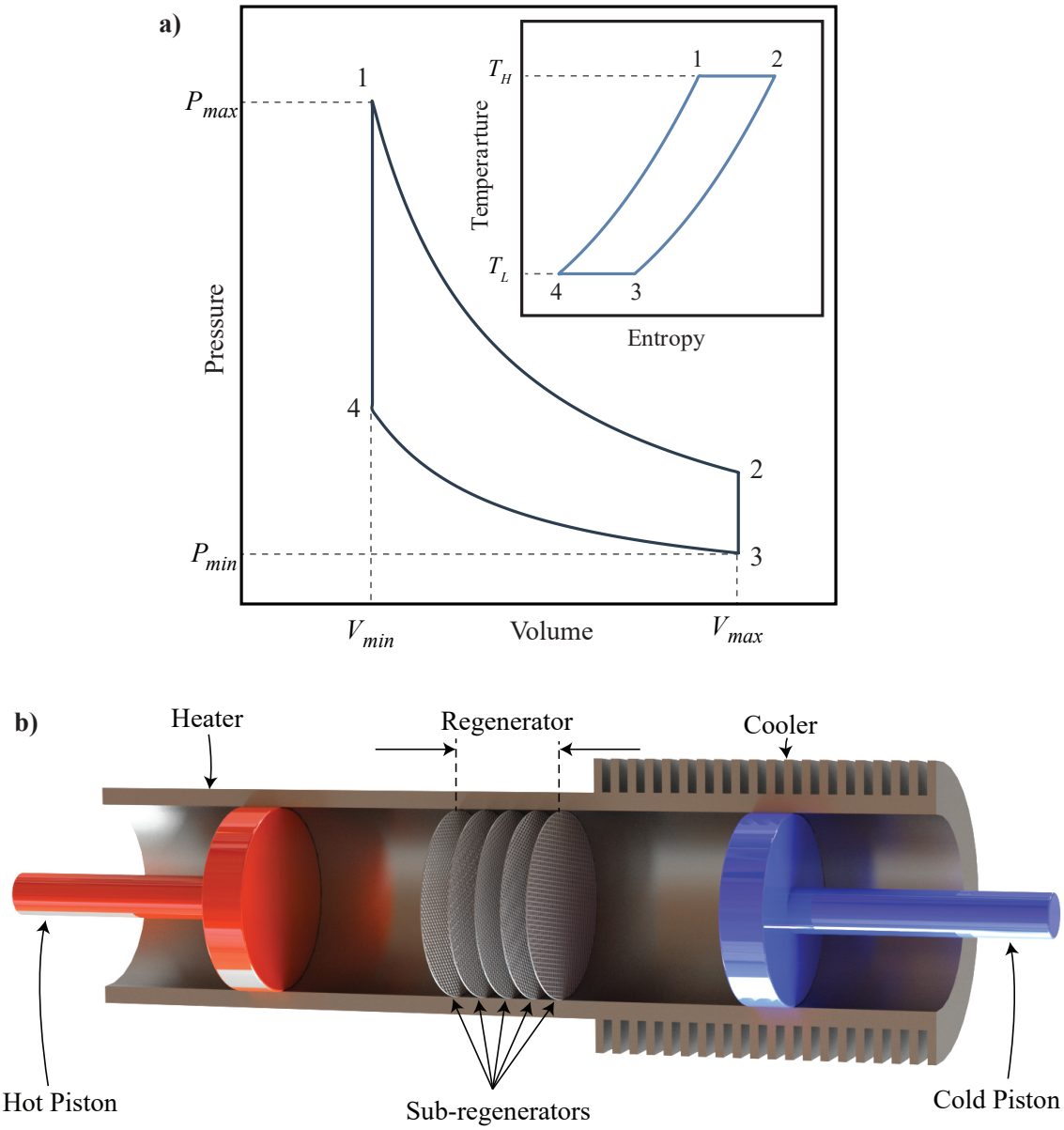

Figure 1.2: **a)** Pressure-volume diagram of the Stirling cycle in main plot and temperature-entropy diagram in inset plot demonstrating isothermal heat addition (1-2), isochoric regenerative cooling (2-3), isothermal heat rejection (3-4), and isochoric regenerative heating (4-1); **b)** Schematic of a Stirling engine with a regenerator composed of 5 sub-regenerators, a hot piston, cold piston, heater, and cooler.

Isothermal heat addition (1-2)

In the isothermal heat addition process, heat is provided by an external fuel source, which is then transferred to the working fluid at a constant temperature. Accordingly,

the hot piston moves to the left and increases the volume of the working fluid, the cold piston remains stationary, and the pressure decreases to satisfy the ideal gas law, as shown in Figure 1.3. The isothermal heat addition process is the expansion stroke of the Stirling cycle, and is therefore the work-output stage.

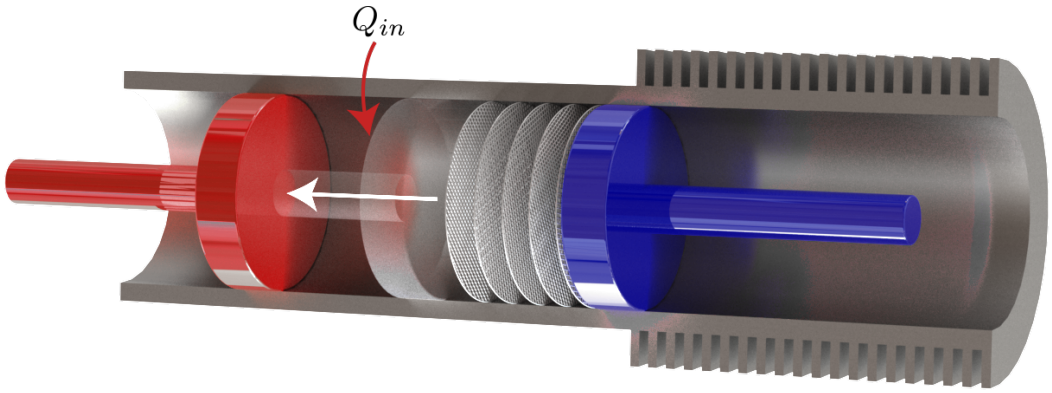

Figure 1.3: Schematic of the isothermal heat addition process in the Stirling cycle.

Isochoric regenerative cooling (2-3)

Following isothermal heat addition is the isochoric regenerative cooling process, where the regenerator absorbs thermal energy from the working fluid to decrease the working fluid's temperature before it enters the cooler for isothermal heat rejection. This process occurs at a constant volume, and therefore decreases the pressure of the working fluid, and both the hot and cold pistons move to the right at the same velocity, which is shown in Figure 1.4.

Isothermal heat rejection (3-4)

In the isothermal heat rejection process, heat is rejected from the working fluid by the cooler and into the surrounding environment at a constant temperature. The cold

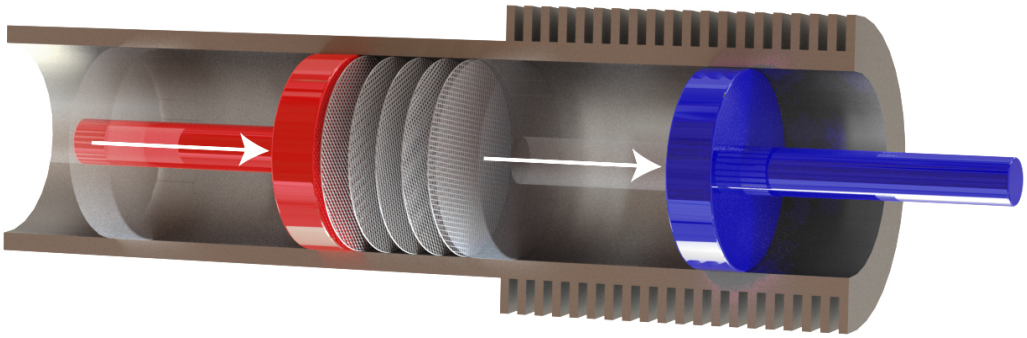

Figure 1.4: Schematic of the isochoric regenerative cooling process in the Stirling cycle.

piston compresses the working fluid as it moves to the left, the hot piston now remains stationary, and the pressure of the working fluid increases as the volume decreases, as shown in Figure 1.5. The isothermal heat rejection process is the compression stroke of the Stirling cycle, and is therefore the work-input stage.

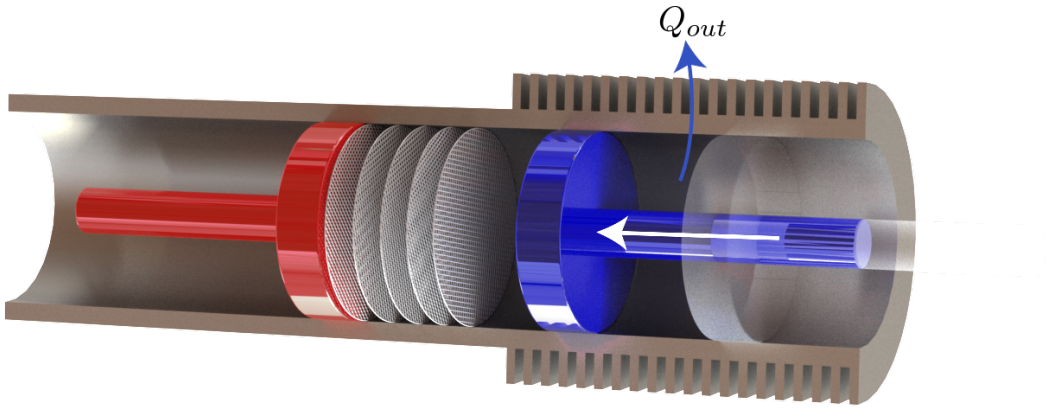

Figure 1.5: Schematic of the isothermal heat rejection process in the Stirling cycle.

Isochoric regenerative heating (4-1)

Finally, the isochoric regenerative heating process occurs, where the regenerator now returns thermal energy to the working fluid to increase the working fluid's temperature before it enters the heater for isothermal heat addition. Again, this process occurs

at a constant volume, but now the pressure of the working fluid increases as its temperature increases, and both the hot and cold pistons move to the left at the same velocity, which is shown in Figure 1.6. This cycle is repeated continuously as the Stirling engine is in operation.

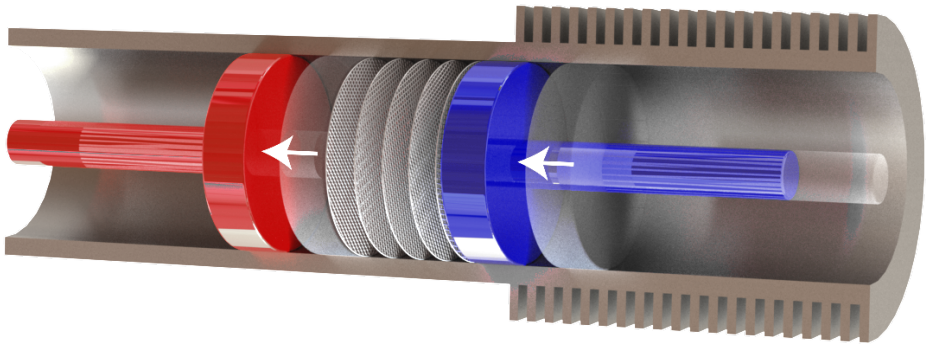

Figure 1.6: Schematic of the isochoric regenerative heating process in the Stirling cycle.

1.2.2 Importance of the regenerator

The regenerator plays a crucial role in the Stirling cycle, and its importance cannot be overstated. Ideally, the regenerator allows the working fluid in the Stirling engine to alternate between target temperatures, T_H and T_L, without any supplemental heat addition or rejection from the engine's heater or cooler, respectively. It accomplishes this task by absorbing and returning thermal energy to the working fluid between the isothermal expansion and compression strokes, which enables the Stirling cycle to theoretically attain the highest possible efficiency (Carnot efficiency). An additional requirement of the regenerator is to minimize the resultant pressure drop of the working fluid as it flows through the regenerator, since an increasing pressure drop

corresponds to a decrease in Stirling engine performance. Thus, designing a regenerator such that it can sustain a sufficient temperature distribution while minimizing the resultant pressure drop is critical to enhancing the performance and efficiency of Stirling engines.

In practice, however, Stirling engines do not attain Carnot efficiency, which is a consequence of the irreversibilities (friction, etc.), the sinusoidal motion of the hot and cold pistons [5], and a regenerator design that produces a substantial pressure drop and an insufficient temperature distribution. The GPU-3 Stirling engine, which is shown in Figure 1.7, implemented a regenerator composed of 308 stacked stainless steel wire mesh sub-regenerators [4, 6]. Such a high value of the number of sub-regenerators requires a considerable amount of regenerator material, which inhibits the flow of the working fluid and leads to higher pressure drops, ultimately reducing the performance and efficiency of Stirling engines. This was observed in the GPU-3 Stirling engine, where the predicted Carnot efficiency was approximately 71%, while the actual efficiency was 27.2% [4, 6]. Other researchers have implemented continuous channel regenerators to reduce the resultant pressure drop, however, this thesis demonstrates that the maximum effectiveness a single regenerator can attain is 50%. Thus, it is important to design regenerators such that they complete the necessary heat exchange to attain a high effectiveness, while limiting the resultant pressure drop to enhance Stirling engine performance and efficiency. It has been evidenced that designing a regenerator to attain a high effectiveness with a correspondingly low pressure drop is challenging and multivariate, therefore extensive research has been performed to develop a better understanding of how regenerators function, and have

sought to quantify the heat transfer rate and resultant pressure drop of the working fluid through the regenerator.

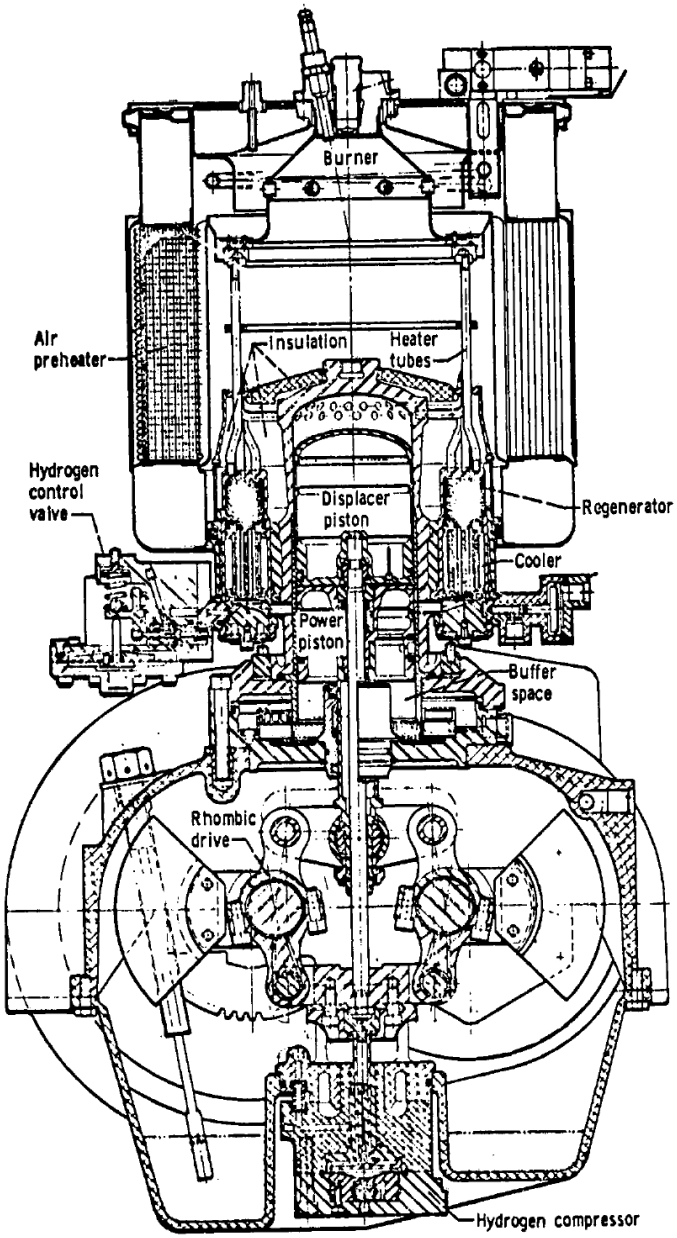

Figure 1.7: Cross section of the GPU-3 Stirling engine. [4]

1.3 Regenerator literature review

This section highlights the past literature that has examined various aspects of Stirling engine regenerators. It begins by summarizing the empirical studies that have developed correlations to calculate the friction factor and Nusselt number for regenerators by using experiments and/or numerical simulations. Research that has investigated the theoretical influence of regenerator effectiveness on Stirling engine performance and efficiency is then presented, followed by a review of the experimental studies that have examined the effects of regenerator material composition and geometry on the performance and efficiency of Stirling engines. Subsequently, a review of the heat transfer models that were developed to quantify regenerator effectiveness based on the regenerator's heat transfer and flow characteristics is presented. Finally, the gaps in the literature are then summarized, and avenues for potential research are introduced.

1.3.1 Empirical studies

Experiments

Experimental studies have used steady and oscillatory flow conditions to develop empirical correlations for the friction factor and Nusselt number for wire mesh sub-regenerators to predict the resultant pressure drop and heat transfer rate. Tanaka et al. [7] conducted oscillatory flow experiments of wire mesh sub-regenerators, and developed empirical correlations for the friction factor and Nusselt number as a function of the Reynolds number, and were therefore able to estimate the heat transfer

rate and pressure drop for various regenerator sizes and flow velocities. Isshiki et al. [8] performed a similar investigation, instead for a higher range of Reynolds numbers (Re $>$ 300), and determined that the friction factor in a decelerating flow is higher than that in an accelerating flow at certain Reynolds numbers, and new empirical correlations for the friction factor and Nusselt number were developed. Rather than performing an oscillatory flow analysis, Sodre et al. [9] conducted a steady flow experiment to investigate wire mesh sub-regenerators, and developed additional empirical correlations to approximate the resultant pressure drop across a stack of wire mesh sub-regenerators. Yamashita et al. [10] built upon the previous studies to examine the effects of the entrance and exit areas on the pressure drop, friction factor, and velocity distribution in wire mesh sub-regenerators, and revealed that the uniformity of the velocity profile is only dependent on the size of the entrance and exit areas of the flow channel, and not on the mesh size or Reynolds number. They also developed a numerical model to predict the velocity profile in the regenerator channel, which was validated with the obtained experimental results. A study performed by Yu et al. [11] investigated the heat transfer characteristics in a Stirling engine regenerator that was subjected to oscillatory flow conditions and an imposed axial temperature gradient by using Planar Laser Induced Fluorescence (PLIF) and Particle Image Velocimetry (PIV) measurement techniques to record the transient temperature and velocity fields. These studies have provided valuable information in regards to the heat transfer and fluid flow characteristics in Stirling engine regenerators, but have not elucidated how they influence regenerator effectiveness.

Experiments and numerical simulations

With the advancement of computational techniques, some studies have used experiments and numerical simulations in tandem to investigate the heat transfer and fluid flow in Stirling engine regenerators. Costa et al. [12] coupled experiments and numerical simulations to conduct a preliminary investigation of the pressure drop and heat transfer characteristics of Stirling engine regenerators, and developed empirical correlations for the friction factor as a function of the Reynolds number. The studies performed by Xiao et al. [13, 14] used experiments and simulations to examine the characteristics of wire mesh sub-regenerators in both oscillatory and steady flow conditions, and determined that within certain ranges of Reynolds number, steady and oscillatory flow conditions share the same friction factor correlation. From these studies, good agreement was demonstrated between the experimental results and numerical simulations, thus revealing the capabilities and accuracy of computational software when examining the Stirling engine regenerator's heat transfer and flow features.

Numerical simulations

Studies have become increasingly independent of experiments since they are taxing and expensive to design and construct, therefore researchers have conducted purely numerical studies to examine the heat transfer and fluid flow characteristics of Stirling engine regenerators, and have validated their models using the experimental results obtained in previous studies. Costa et al. [16] conducted a numerical analysis to quan-

tify the pressure drop through a Stirling engine regenerator composed of multiple wire mesh sub-regenerators, and validated their simulations using the experimental results obtained by Tanaka et al. [7] with less than 5% deviation, and new empirical correlations for the friction factor were developed for various regenerator sizes. Costa et al. [17] then undertook a similar investigation and developed empirical correlations for the Nusselt number to compute the convective heat transfer rate for wire mesh sub-regenerators in different configurations. Costa et al. [15] then presented a stepwise numerical methodology for the development of the flow resistance and convective heat transfer coefficient in wire mesh sub-regenerators to model the regenerator as a porous media to simplify and reduce computing time for multi-dimensional Stirling engine simulations. Figures from the study performed by Costa et al. [15] are shown in Figure 1.8. A study conducted by Barreno et al. [18] derived empirical correlations for the pressure drop and heat transfer rate for wire mesh sub-regenerators under developing oscillatory flow conditions, and found good agreement between their numerical simulations and the experimental results obtained in Zhao and Cheng's study [19].

It has been shown that significant work has been completed to quantify the thermal and flow features of conventional wire mesh sub-regenerators, however, other research has focused on developing and testing different regenerator configurations, such as continuous regenerators, to determine if they have superior heat transfer and flow characteristics in comparison to conventional wire mesh sub-regenerators. Alfarawi et al. [20] used a computational approach to examine the fluid flow and heat transfer characteristics in miniature-channel regenerators, and demonstrated that the

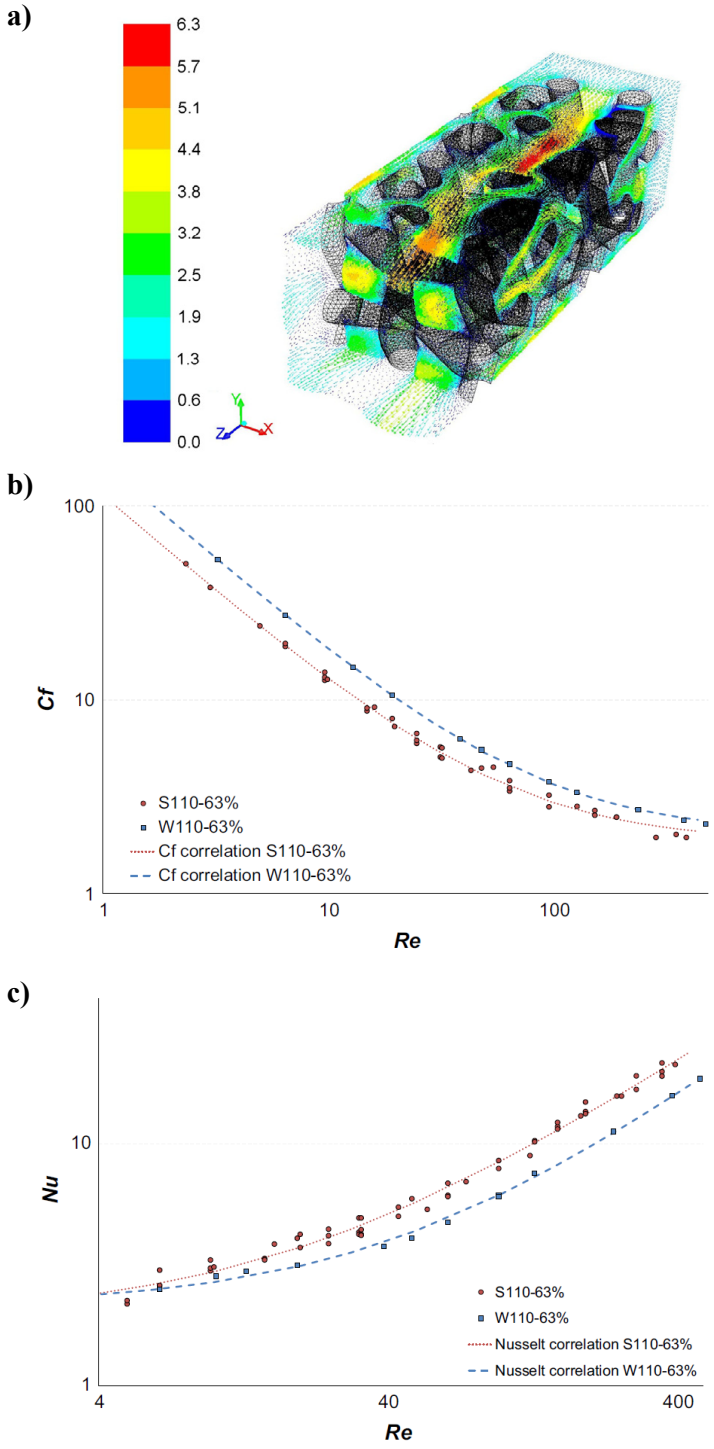

Figure 1.8: **a)** Velocity vectors coloured by velocity magnitude (m/s) of working fluid flowing through wire mesh sub-regenerators; **b)** Friction coefficient correlations as a function of Reynolds number; **c)** Nusselt number correlations as a function of Reynolds number. [15]

axial conduction in the regenerator produced adverse effects due to the low temperature distribution, as shown in Figure 1.9(a). Their study also revealed that minimizing axial conduction losses can be accomplished by selecting a regenerator material with a high volumetric heat capacity and a low thermal conductivity. A further study performed by Alfarawi et al. [21] used a combined experimental and numerical analysis to quantify the heat transfer and flow friction in miniature-channel regenerators, and developed empirical correlations for the friction factor and Nusselt number, which is shown in Figure 1.9(b). Li et al. [22] examined the fluid flow and heat transfer characteristics of hexagonal channel regenerators by using numerical simulations that were experimentally validated, and determined that the hexagonal microchannels perform significantly better in comparison to conventional wire mesh sub-regenerators due to lower frictional losses and higher heat transfer rates. Furthermore, Li et al. [23] derived analytical approximations for the heat transfer characteristics in hexagonal channel regenerators under oscillatory flow conditions in the thermal entrance region, and validated their analytical model with the results obtained from the previous study [22]. Tew el al. [24] developed an involute-foil regenerator design, which was compared against an assortment of regenerator configurations, and developed empirical correlations for the friction factor and Nusselt number as a function of the Reynolds number. The work that has been completed to quantify the thermal and flow characteristics of various regenerator configurations has proven to be valuable since the heat transfer rate and resultant pressure drop can be calculated for a wide range of flow cases using the developed empirical correlations. However, these studies have neglected to examine how these parameters influence the effectiveness of regenerators

and the performance of Stirling engines.

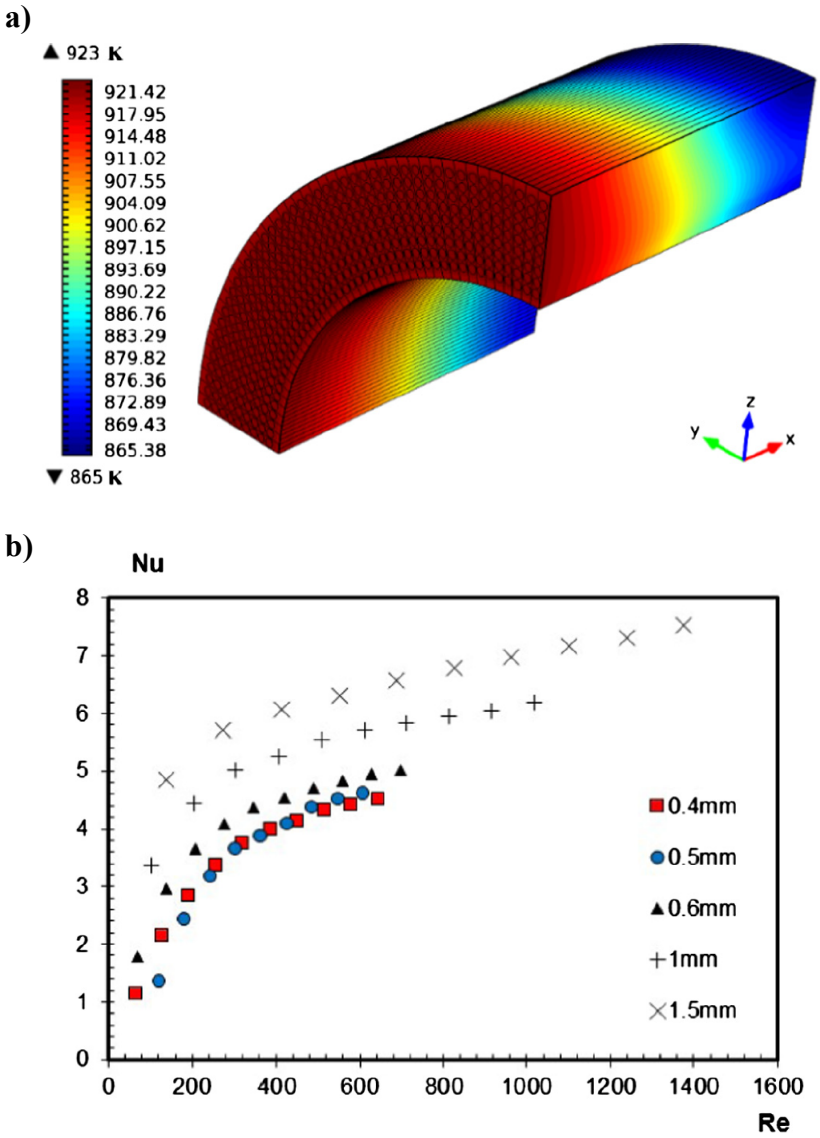

Figure 1.9: **a)** Temperature contours for 1.5 mm channel regenerator at Stirling engine rotational speed of 1000 rpm and time of 30 s of operation; **b)** Nusselt of various channel regenerators as a function of the Reynolds number. [21]

1.3.2 Influence of regenerator effectiveness

Conversely, some studies have defined a value for the regenerator effectiveness without investigating the parameters that could influence this value. Costa et al. [25]

performed a comparison between the Stirling and Ericsson cycles to determine which produced greater net work outputs in certain situations, and assumed ideal regeneration in their analysis. Blank et al. [26] conducted a power optimization analysis of the Stirling cycle assuming ideal regeneration, and developed relations to predict the maximum power output of the Stirling engine. Ahmadi et al. [27] assumed ideal regenerator effectiveness and performed an optimization analysis of the Stirling engine, where the key parameters they investigated were the engine's volumetric ratio, the heat source temperature, and the product of the convective heat transfer coefficient and regenerator surface area.

Other studies have defined a value for the regenerator effectiveness to examine how it influences the efficiency of Stirling engines. Thombare et al. [28] conducted a theoretical analysis of an α-type Stirling engine to determine the influence of the regenerator effectiveness and working fluid properties on Stirling engine efficiency, and revealed that a decreasing regenerator effectiveness corresponds to a decreasing Stirling engine efficiency. Kontragool et al. [29] adjusted the value of the regenerator effectiveness in their theoretical model to investigate its influence on Stirling engine efficiency, and determined that in order for the Stirling engine to attain a high efficiency, a good regenerator is needed. Kaushik et al. [30] conducted a finite time thermodynamic analysis of a Stirling engine and adjusted the value of the regenerator effectiveness, and found that the regenerator effectiveness only has an influence on the Stirling engine's efficiency and not its power output. Examining the influence of the regenerator effectiveness on Stirling engine efficiency is important, however, these studies do not discuss the parameters that could impact the regenerator's effective-

ness or Stirling engine efficiency, nor do they suggest how to design a regenerator to attain a desired effectiveness.

1.3.3 Experimental Stirling engine performance studies

Experimental studies have tested an assortment of regenerator materials and geometric configurations to examine their influence on Stirling engine performance and efficiency. Gheith et al. [31] conducted an experimental performance analysis to assess the influence of regenerator material composition on the power output of a 500 W Stirling engine. The study evaluated four different wire mesh sub-regenerator materials (stainless steel, copper, aluminum, and Monel 400) and demonstrated that stainless steel provides the highest Stirling engine power output in comparison to the remaining materials. They also determined that the use of copper is not recommended since it can oxidize, thus diminishing its ability to exchange thermal energy with the working fluid, and decreases the power output of the Stirling engine. Gheith et al. [32] conducted a similar experimental analysis using the same Stirling engine, which is shown in Figure 1.10, by evaluating the same four regenerator materials, but also considered the regenerator's porosity. The study assessed five different regenerator porosities (75%, 80%, 85%, 90%, and 95%) and determined that a porosity of 85% maximized their Stirling engine's performance and minimized the heat transfer and flow friction losses. Chen et al. [33] conducted an experimental analysis of a regenerator in a γ-type Stirling engine to investigate the influence of regenerator material, wire mesh sub-regenerator arrangement, regenerator wire diameter, and fill

factor. The study determined that copper generated a higher Stirling engine power output due to its higher thermal conductivity in comparison to stainless steel, and also found that aligning the wire mesh sub-regenerators such that they are normal to the flow direction is advantageous in comparison to parallel arrangements. This study also revealed an optimum fill factor that maximizes their Stirling engine's performance, and found that a larger gap size between wires reduced the pressure drop of the working fluid, thus increasing the performance of the Stirling engine. Takizawa et al. [34] conducted an experimental comparison between conventional wire mesh sub-regenerators and a novel regenerator design they developed for the study, and found that the novel design enhanced the performance and efficiency of their Stirling engine. The study by Abduljalil et al. [35] compared four different regenerator materials and geometric configurations, including a cellular ceramic substrate with regular square channels, packed steel scourers, stainless steel wool, and regular wire mesh sub-regenerators. They determined that the stainless steel wool and packed scourers performed significantly worse in comparison to the conventional wire mesh sub-regenerators, but found that the ceramic substrate with square channels could provide an alternative to traditional configurations due to the reduced resultant pressure drop. The aforementioned experimental performance studies have illuminated some of the key regenerator parameters that influence the performance and efficiency of Stirling engines, namely regenerator material composition and geometry. However, there is no consensus amongst these studies that recommend an ideal material or a particular geometry that should be implemented in Stirling engines to maximize their power output. This is perhaps a consequence of the nature of these studies, where

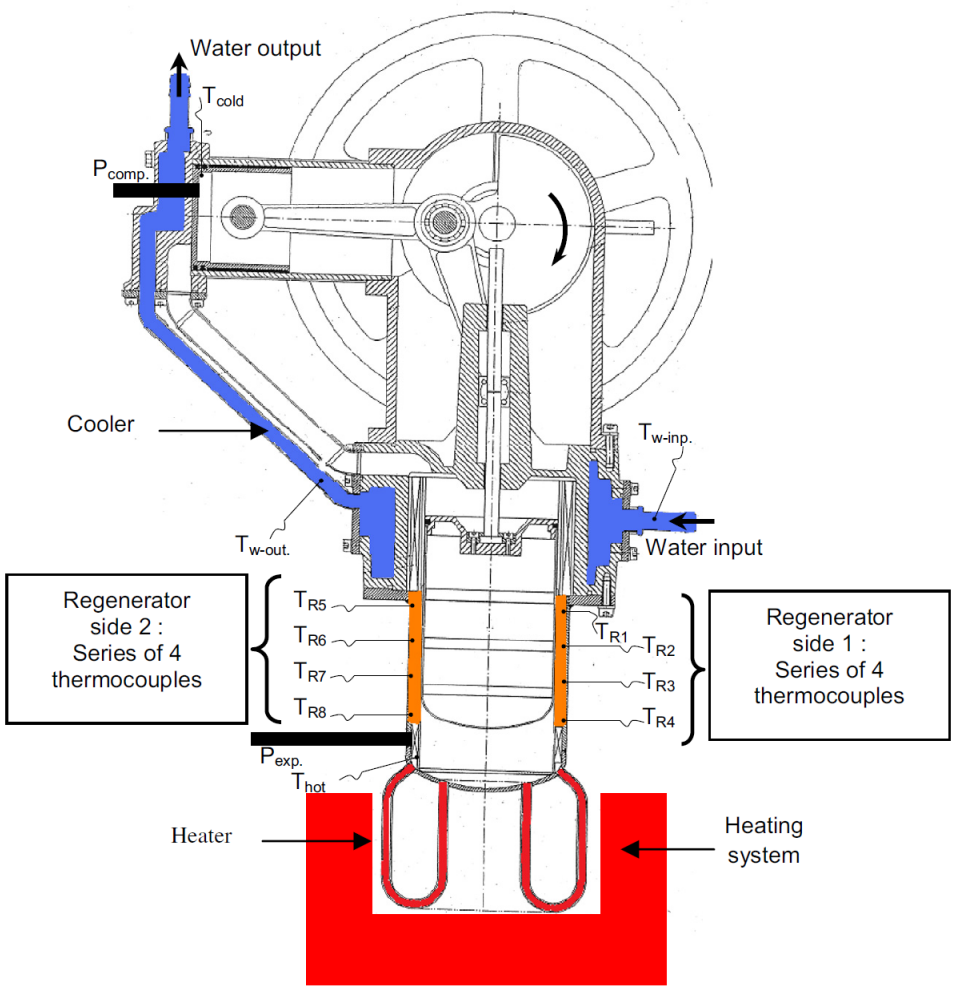

Figure 1.10: Schematic of the Stirling engine used in the studies performed by Gheith et al. [31, 32]

each individual Stirling engine has its own preferred regenerator specifications that will maximize the engine's performance and efficiency, but are not transferrable to other Stirling engines. Additionally, these studies do not quantify the influence of the investigated parameters on the effectiveness of regenerators.

1.3.4 Regenerator heat transfer models

Researchers have developed heat transfer models of regenerators that consider various physical parameters to calculate their effectiveness, and can apply to all Stirling engines. A study performed by Klein et al. [36] developed an analytical model to determine the effectiveness of continuous counterflow regenerators, and revealed that the key parameters that must be enhanced to attain a high regenerator effectiveness are the number of transfer units and Peclet number. Organ et al. [37] developed a heat transfer model that accounts for the oscillatory motion of the working fluid, the geometry of the wire mesh sub-regenerators, and the flow friction effects to approximate the ineffectiveness of the regenerator, and quantified the influence of the number of transfer units and flushing ratio on the ineffectiveness of the regenerator. Monte et al. [38] built upon the aforementioned study and developed an "easy-to-handle" expression for the effectiveness of the regenerator as a function of the number of transfer units and flush ratio by generating an analytical solution to the one-dimensional heat transfer processes. Trevizoli et al. [39] conducted a theoretical analysis of Stirling engine regenerators by implementing an entropy generation minimization technique to enhance the effectiveness of regenerators. Chen et al. [40] developed a computational code to examine the influence of a moving regenerator on the performance of a β-type Stirling engine, and found that the moving regenerator acts as an effective thermal barrier between the Stirling engine's heater and cooler, but found that it introduces a significant pressure drop that would hinder the Stirling engine's performance. A study conducted by Jones [41] examined the effects of the regenerator thermal mass

ratio on the ineffectiveness of the regenerator and the power loss factor of the Stirling engine. The work found that regenerator thermal mass ratio values between 20:1 and 40:1 can influence the performance of Stirling engines, and was not concerned with recommending an ideal value for the regenerator thermal mass ratio. Dai et al. [42] theoretically showed that a regenerator must have an unevenly distributed temperature to attain an effectiveness greater than 50%, and that an unevenly distributed temperature can be accomplished by using a number of smaller heat reservoirs to divide the regenerator into sub-regenerators.

1.3.5 Gaps in the literature

Aside from the study completed by Dai et al. [42], there has been no work that has provided insight into designing regenerators such that they can attain a desired effectiveness. There have been studies that have quantified the resultant pressure drop and heat transfer rate in Stirling engine regenerators, but have placed no emphasis on relating these parameters to regenerator effectiveness. Other studies have defined a value for the regenerator effectiveness in their analysis without considering the variables that could influence this value. Furthermore, the experimental performance studies have implemented a trial-and-error methodology to determine the optimum regenerator parameters to maximize Stirling engine performance, however, the shortcomings of this approach are that the optimum values for the regenerator's design varied for each individual Stirling engine. Additionally, the regenerator's effectiveness was not quantified in each of these studies. In the studies that developed heat trans-

fer models of the regenerator, it has been evidenced that enhancing the number of transfer units is critical to improving regenerator effectiveness. However, the number of transfer units is dependent on the convective heat transfer coefficient and mass flow rate of the working fluid, which are predominantly a function of the Stirling engine's rotational speed, and are therefore parameters that cannot be considered in the regenerator's physical design. Dai et al. [42] and Jones [41] have stressed the importance of the regenerator's physical parameters on its effectiveness, more specifically, the number of sub-regenerators and regenerator thermal mass ratio, respectively. Therefore, it is critical that the influence of the regenerator thermal mass ratio and number of sub-regenerators are investigated in tandem to elucidate the parameters that have an impact on regenerator effectiveness, and to design regenerators such that they can attain a desired effectiveness to enhance the efficiency of Stirling engines.

To date, there has not been any research that has determined the required values for the regenerator thermal mass ratio and number of sub-regenerators to attain a specific regenerator effectiveness, and especially doing so without employing unnecessarily high values of each and generating higher pressure drops. The understanding of how to select these values will lead to enhanced regenerator designs capable of attaining a high effectiveness while producing low pressure drops, and will improve the performance and efficiency of Stirling engines.

1.4 Thesis objectives

The objective of this thesis is to provide Stirling engine designers with the necessary tools to produce regenerators with a high effectiveness that will enhance the efficiency of Stirling engines. Therefore, the scope of this thesis is to accomplish the following:

- Determine the settling temperature of the regenerator and working fluid for regenerators composed of single and multiple sub-regenerators;
- Determine which parameters have an influence on the effectiveness of regenerators, and which can be neglected;
- Derive expressions for the regenerator effectiveness and Stirling engine efficiency as a function of the important parameters;
- Determine the sub-regenerator mass distribution that corresponds to maximum regenerator effectiveness;
- Experimentally validate the heat transfer model.

1.5 Thesis organization

The remainder of this thesis begins at Chapter 2, which describes the mathematical modelling of a regenerator and working fluid inside of a Stirling engine. This chapter reveals the parameters that influence the effectiveness of regenerators, and develops a heat transfer model to determine the settling temperature of the working fluid and regenerator composed of multiple sub-regenerators. Additionally, expressions for

regenerator effectiveness are derived, and the development of the Stirling engine efficiency model is presented. Chapter 3 provides a description of the experimental apparatus and methodology used to gather data to validate the aforementioned heat transfer model. Chapter 4 is the results and discussion section of this thesis, where the influence of the regenerator thermal mass ratio and number of sub-regenerators on Stirling engine efficiency is quantified, and insight into designing regenerators such that they can attain a desired effectiveness is demonstrated. Additionally, this chapter reveals the sub-regenerator mass distribution that provides maximum regenerator effectiveness, and the heat transfer model and the assumptions made are then experimentally validated. Finally, in Chapter 5, the conclusions of this thesis are summarized, recommendations for future study are presented, and the contributions of this thesis are described.

Chapter 2

Mathematical modelling

2.1 Transient heat transfer model of a single regenerator

In order to determine the thermal behaviour of a regenerator in a Stirling engine, a single regenerator (one sub-regenerator) along with the working fluid are initially modelled during the two isochoric (constant volume) regeneration processes of the Stirling cycle. During these processes, energy is exchanged between the working fluid and the Stirling engine's regenerator, which is shown in Figure 1.2, and their temperatures change conversely to one another. This means that an incremental increase of energy in one of the mediums must be balanced by the decrease of energy in the other, which is expressed as:

$$-m_r c_r \left(T_r^{p+1} - T_r^p\right) = m_f c_{v,f} \left(T_f^{p+1} - T_f^p\right) \tag{2.1}$$

where superscript p denotes the current time step, and $p+1$ denotes the successive

step. The rate of energy change must also be balanced, such that the rate of heat transfer in the regenerator is equal to the convection at the surface of the regenerator. Local thermal equilibrium is assumed within the regenerator material and working fluid, thus neglecting local conduction heat transfer within each medium, resulting in:

$$\rho V c_r \frac{dT_r}{dt} = hA\left(T_f - T_r\right) \tag{2.2}$$

For thermal equilibrium to be valid for the working fluid, sufficient mixing and small length scales are required, which is expected in Stirling engine regenerators. To ensure that the thermal equilibrium approximation is valid for the solid regenerator material, the following condition must be satisfied:

$$\frac{hr}{2k_r} < 0.1 \tag{2.3}$$

That is, the Biot number must be below the threshold value of 0.1 [43]. The largest expected value of the Biot number for the work analyzed in this thesis corresponds to the regenerator material with the lowest thermal conductivity (stainless steel: $k_r = 16.2$ W/mK), the largest radius ($r = 0.04$ mm), and the highest heat transfer coefficient ($h = 18,000$ W/m^{2}K), which results in a value of 0.022. Since this is below the threshold value, the approximation will be valid. The regenerator material properties are assumed to be constant in this analysis, and the properties of the employed working fluid are evaluated at the arithmetic mean of target temperatures, T_H and T_L.

To model the transient thermal response of the working fluid and regenerator, Equation (2.2) was discretized as follows:

$$\rho V c_r \left(\frac{T_r^{p+1} - T_r^p}{\Delta t} \right) = hA \left(T_f^p - T_r^p \right) \tag{2.4}$$

Assuming that the regenerator is made up of a cylindrical material, where the length is substantially larger than the radius, the characteristic length scale of the regenerator is $V/A = r/2$, and Equation (2.4) is simplified to:

$$T_r^{p+1} = \frac{2h\Delta t}{\rho c_r r} T_f^p + \left(1 - \frac{2h\Delta t}{\rho c_r r} \right) T_r^p \tag{2.5}$$

Equation (2.1) is then rearranged as follows:

$$T_f^{p+1} = T_f^p - \gamma \left(T_r^{p+1} - T_r^p \right) \tag{2.6}$$

where the regenerator thermal mass ratio, γ, is:

$$\gamma = \frac{m_r c_r}{m_f c_{v,f}} \tag{2.7}$$

Equations (2.5) and (2.6) model the thermal response of the regenerator and working fluid, respectively, and they reveal that the parameters that influence the transient response of the system are the radius of the regenerator, r, material properties of the regenerator, c_r and ρ, the heat transfer coefficient, h, and the regenerator thermal mass ratio, γ. The value of the time step, Δt, was set low enough to maintain stability of the simulation and to ensure it did not influence the temperatures. To examine

how each of the parameters influence the settling temperature of the regenerator and working fluid, a parametric analysis was undertaken.

2.2 Transient parametric analysis for a single regenerator

A parametric analysis of the transient heat transfer model was conducted for a single regenerator (one sub-regenerator) to reveal how the temperatures of the regenerator and working fluid are impacted by the regenerator radius, heat transfer coefficient, material properties, and regenerator thermal mass ratio. The regenerator radius, material, and heat transfer coefficient were varied in Figures 2.1(a)-(c) to assess how they impact the settling temperature of the system, which is the settling temperature of both the regenerator and working fluid. The influence of the regenerator thermal mass ratio, γ, was then examined in Figure 2.1(d). The values were chosen based on the specifications of a GPU-3 Stirling engine [4, 6], which has a stainless steel regenerator with a wire radius of $r = 0.02$ mm, and a heat transfer coefficient of approximately $h = 18{,}000$ W/m^{2}K was calculated for the entire regenerator mesh, using [44]:

$$\mathrm{Nu} = \frac{hD}{k_f} = C_2 C_1 \mathrm{Re}^b \mathrm{Pr}_{avg}^{0.36} \left(\frac{\mathrm{Pr}_{avg}}{\mathrm{Pr}_r} \right)^{\frac{1}{4}} \tag{2.8}$$

A regenerator thermal mass ratio of $\gamma = 5{:}1$ was selected for the plots in Figures 2.1(a)-(c) to illustrate the influence of these parameters on the regenerator and working fluid settling temperatures, and the value of γ was then varied for Figure 2.1(d). The

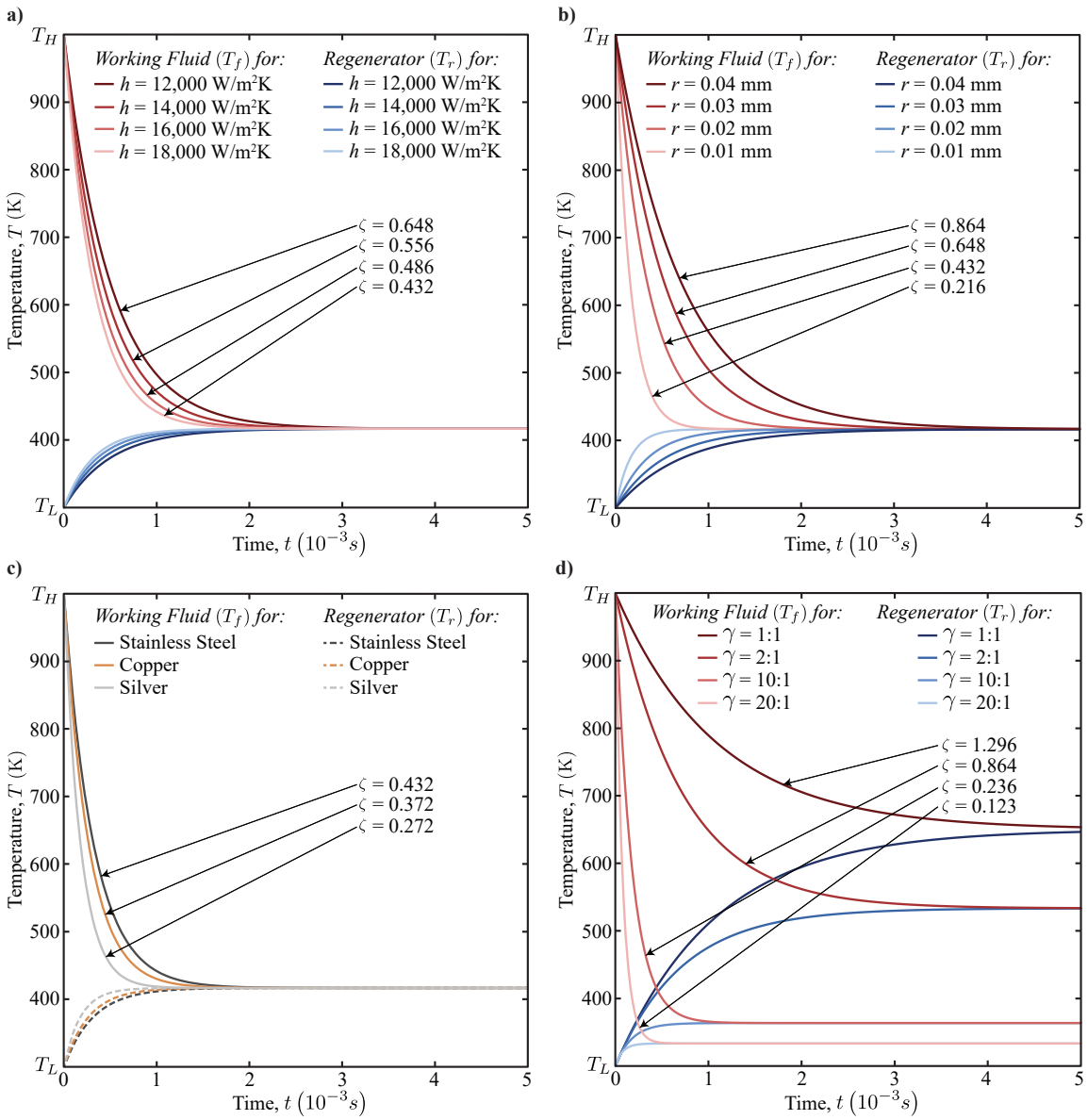

Figure 2.1: Transient response of a single regenerator (one sub-regenerator) absorbing energy from the working fluid for: **(a)** varying h with constant $r = 0.02$ mm, constant regenerator material (stainless steel), and constant $\gamma = 5{:}1$, **(b)** varying r with constant $h = 18{,}000$ W/m^{2}K, constant regenerator material (stainless steel), and constant $\gamma = 5{:}1$, **(c)** varying regenerator material with constant $r = 0.02$ mm, constant $h = 18{,}000$ W/m^{2}K, and constant $\gamma = 5{:}1$, and **(d)** varying γ, constant $r = 0.02$ mm, constant $h = 18{,}000$ W/m^{2}K, and constant regenerator material (stainless steel).

results from a regeneration process of a single sub-regenerator with air moving from hot ($T_H = 1000$ K) to cold ($T_L = 300$ K) are plotted in Figures 2.1(a)-(c), and they

reveal that the heat transfer coefficient, radius, and material have an impact on the rapidity of the transient response but have no influence on the settling temperature of an individual cycle. The GPU-3 Stirling engine operates at rotational speeds at or below a value of 3,500 rpm [4, 6], which corresponds to a minimum regeneration time of approximately 0.004 s. The settling time in Figures 2.1(a)-(c) is a maximum of 0.004 s, which indicates that the regenerator temperature will reach the equilibrium temperature during each regeneration process. Therefore, in these cases, the settling time is irrelevant and these parameters will not have an influence on the effectiveness of the regenerator or performance of the engine. The only way to influence the regenerator's effectiveness is to change the value of the settling temperature, which can be accomplished by varying the remaining parameter, the regenerator thermal mass ratio.

The response of four different regenerator thermal mass ratios were plotted in Figure 2.1(d) for a regeneration process with air moving from hot ($T_H = 1000$ K) to cold ($T_L = 300$ K), and it is shown that the regenerator thermal mass ratio not only impacts the rapidity of the system response, but also the system settling temperature. The value of the system settling temperature is an important consequence of the regenerator thermal mass ratio since it indicates how much additional thermal energy the heater and cooler of the Stirling engine must either add or reject, respectively, to attain target temperatures, T_H and T_L.

Not all Stirling engines operate at 3,500 rpm, and it is desirable to ensure that the regenerator has the necessary specifications to exchange thermal energy with the working fluid within the given time frame determined by the engine's rotational speed.

To do this, we must compare the natural time scale for regeneration, τ, and the time available in the cycle for regeneration to occur, t_{reg}. The natural time scale can be obtained from Equations (2.5) and (2.6) and is expressed as follows:

$$\tau = \frac{\rho c_r r}{2h\,(1+\gamma)} \tag{2.9}$$

The time available for regeneration to occur is one quarter of a rotation in the Stirling cycle, which is calculated as:

$$t_{reg} = \frac{15}{\omega} \tag{2.10}$$

Equation (2.9) corresponds to the time when the regenerator and working fluid temperatures are within 63.2% of the system settling temperature, and we must therefore multiply the natural time scale by 5 to ensure that they are within 99% of the system settling temperature, hence:

$$5\tau = \frac{5}{2}\frac{\rho c_r r}{h\,(1+\gamma)} \tag{2.11}$$

To ascertain that there is sufficient time for regeneration to occur, the following is evaluated:

$$\frac{5\tau}{t_{reg}} < 1 \tag{2.12}$$

which results the following expression, denoted as ζ:

$$\zeta = \frac{\omega \rho c_r r}{6h\,(1+\gamma)} < 1 \tag{2.13}$$

Values of ζ less than one indicate that more than 99% of the available heat is being exchanged within the given window of time, while values greater than one indicate that the regenerator's specifications are inadequate to exchange 99% of the available heat with the working fluid. The ζ values are labelled in Figures 2.1(a)-(d). Stirling engine designers can now evaluate whether or not the regenerator is transferring sufficient thermal energy within the given window of time, and can vary the regenerator's specifications to ensure that they are maximizing the heat transfer between the working fluid and regenerator with the use of Equation (2.13). In summary, Equations (2.3) and (2.13) are the two conditions that must be satisfied to confirm that only the regenerator thermal mass ratio influences the settling temperature of the system for a single regenerator, and correspondingly the effectiveness of the regenerator. Accordingly, a heat transfer model that considers only the regenerator thermal mass ratio is now developed and expanded to the case of a regenerator composed of multiple sub-regenerators.

2.3 Heat transfer model for various numbers of sub-regenerators

Having shown that for a single regenerator the thermal mass ratio is the only valid parameter, the case of multiple sub-regenerators is now examined. To model a re-

generator with multiple sub-regenerators, the assumption that each sub-regenerator behaves as a single regenerator is made, and the whole regenerator is then composed of a series of thermally isolated sub-regenerators. This approximation will be validated by experiments and shown to yield accurate temperature predictions for regenerators with multiple sub-regenerators. Having determined that the regenerator thermal mass ratio is the sole parameter that influences the system settling temperature, only Equation (2.6) is required to model the settling temperature of regenerators composed of a number of sub-regenerators and the working fluid. Since the settling time has been shown to be irrelevant, Equation (2.6) can be rewritten without successive time steps, and the p superscript is replaced with a subscript denoting the *initial* temperature (indicating the temperature at the start of each regeneration process), while the $(p+1)$ superscript is replaced with a subscript denoting the $final$ temperature (indicating the temperature at the end of each regeneration process). The heat transfer model is then simplified by rearranging Eq. (2.6) for a system settling temperature, which is the condition when the working fluid and each sub-regenerator attain the same temperature:

$$T_{sys} = T_{f,final} = T_{r,final} \tag{2.14}$$

and Equation (2.6) becomes:

$$T_{sys} = \frac{T_{f,initial} + \gamma T_{r,initial}}{\gamma + 1} \tag{2.15}$$

Four versions of Equation (2.15) are required to model the system settling temperature

for a regenerator with multiple sub-regenerators. To model one regenerative cooling process, where the regenerator is absorbing thermal energy from the working fluid, the following two equations are required:

$$T_{sys,H}^{(1)} = \frac{T_H + \gamma^{(1)} T_{sys,L}^{(1)}}{\gamma^{(1)} + 1} \tag{2.16}$$

$$T_{sys,H}^{(i)} = \frac{T_{sys,H}^{(i-1)} + \gamma^{(i)} T_{sys,L}^{(i)}}{\gamma^{(i)} + 1} \tag{2.17}$$

where Equation (2.16) is the system settling temperature of the first sub-regenerator for one regenerative cooling process, and Equation (2.17) is the system settling temperature of each of the subsequent sub-regenerators, with their order denoted by the superscript i. To model one regenerative heating process, where the regenerator is returning thermal energy to the working fluid, the following two equations are required:

$$T_{sys,L}^{(N)} = \frac{T_L + \gamma^{(N)} T_{sys,H}^{(N)}}{\gamma^{(N)} + 1} \tag{2.18}$$

$$T_{sys,L}^{(i)} = \frac{T_{sys,L}^{(i+1)} + \gamma^{(i)} T_{sys,H}^{(i)}}{\gamma^{(i)} + 1} \tag{2.19}$$

where Equation (2.18) is the system settling temperature of the N^{th} or last sub-regenerator, and Equation (2.19) is the system settling temperature of each of the subsequent sub-regenerators in reverse order since the working fluid is flowing back through the regenerator. The regenerator thermal mass ratio for each sub-regenerator is a fraction of the total regenerator thermal mass ratio, and in the case of a uniformly distributed mass, each value of $\gamma^{(i)}$ would be equal to γ/N. It should be noted

that modelling a system with one sub-regenerator requires only Equations (2.16) and (2.18). The superscript i, is the sub-regenerator location (i.e. second sub-regenerator, third sub-regenerator, etc.) and N is the total number of sub-regenerators that the regenerator is composed of, where $1 < i < N$.

The operation of a Stirling engine is cyclical, so the regenerative processes described by Equations (2.16)-(2.19) must be repeated over a number of cycles to simulate the thermal behaviour. The Stirling engine and regenerator will reach a steady operating condition after a number of cycles where the system settling temperatures in Equations (2.16)-(2.19) no longer change. To model the cyclical behaviour for a single regenerator, it begins by assuming the working fluid is in the hot side at a temperature of T_H and the regenerator is initially at a temperature of $T^{(1)}_{sys,L} = T_L$. Equation (2.16) is then used for the first regenerative cooling process (which is denoted with n, so for the first one $n = 1$), and substitute the resulting hot system settling temperature ($T^{(1)}_{sys,H}$) into Equation (2.18) to describe the subsequent regenerative heating process ($n = 2$). The resulting cold system settling temperature ($T^{(1)}_{sys,L}$) from Equation (2.18) is then substituted into Equation (2.16) to model the subsequent regenerative cooling process ($n = 3$). This process is repeated and produces the following summation when rearranged for the hot system settling temperature:

$$T^{(1)}_{sys,H} = T_H \sum_{n=1}^{\infty} \frac{\gamma^{2(n-1)}}{(1+\gamma)^{(2n-1)}} + T_L \left(\sum_{n=1}^{\infty} \frac{\gamma^{(2n-1)}}{(1+\gamma)^{2n}} + \frac{\gamma^n}{(1+\gamma)^n} \right) \tag{2.20}$$

To simulate steady operating conditions, the number of regenerator passes is set to infinity ($n = \infty$), which reduces the hot system settling temperature to:

$$T_{sys,H}^{(1)} = T_H \frac{(\gamma+1)}{(2\gamma+1)} + T_L \frac{\gamma}{(2\gamma+1)} \tag{2.21}$$

A similar methodology is used to model regenerators with multiple sub-regenerators using Equations (2.16)-(2.19).

Equations (2.16)-(2.19) are used to calculate a regenerator effectiveness based on the resultant system settling temperatures. Figure 2.2 shows the system settling temperatures for a regenerator with 3 sub-regenerators ($N = 3$) across a complete Stirling

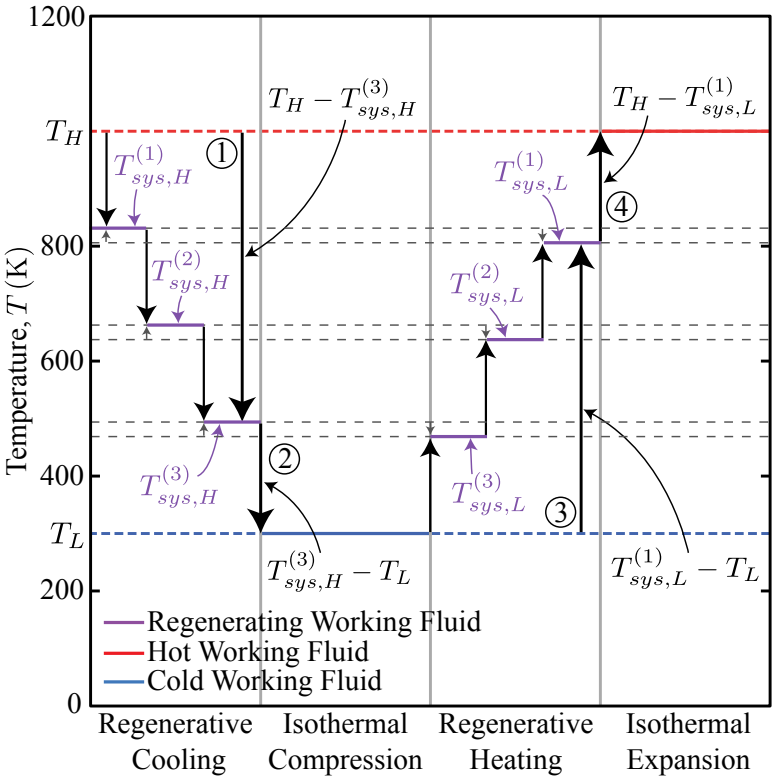

Figure 2.2: Schematic diagram of the heat transfer model once steady engine operation has been reached for one complete Stirling cycle, illustrating the regenerative heating and cooling processes for a regenerator composed of 3 sub-regenerators, $N = 3$, and regenerator thermal mass ratio, $\gamma = 20{:}1$.

engine cycle, where steady engine operation has been reached. The first step is denoted by the circled ① in Figure 2.2, which shows the temperature of the working fluid as the working fluid travels from the hot side through the 3 sub-regenerators. In the first stage of step ① the working fluid and first sub-regenerator temperatures begin at T_H and $T_{sys,L}^{(1)}$ respectively, and the first sub-regenerator absorbs thermal energy from the working fluid resulting in both mediums settling at a temperature of $T_{sys,H}^{(1)}$, which is the regenerative cooling process for the first sub-regenerator. Subsequently, the working fluid travels through the remaining two sub-regenerators, as shown in Figure 2.2, and both the regenerator and working fluid settle at a temperature of $T_{sys,H}^{(3)}$ after the third and final sub-regenerator. The working fluid must attain a temperature of T_L before the subsequent isothermal compression process; therefore, the Stirling engine's cooler must reject an additional amount of thermal energy that is proportional to the remaining temperature difference, $T_{sys,H}^{(3)} - T_L$ (since $N = 3$), which is shown as step ② in Figure 2.2. For the subsequent regenerative heating process, denoted by the circled ③, the working fluid travels from the cold side through the 3 sub-regenerators in reverse order, as shown in Figure 2.2. The working fluid and third sub-regenerator temperatures begin at T_L and $T_{sys,H}^{(3)}$ respectively, and the third sub-regenerator returns thermal energy to the working fluid resulting in both mediums settling at a temperature of $T_{sys,L}^{(3)}$, which is the regenerative heating process for the third sub-regenerator. Subsequently, the working fluid travels through the remaining two sub-regenerators in reverse order, as shown in Figure 2.2, and both the regenerator and working fluid settle at a temperature of $T_{sys,L}^{(1)}$ after the final sub-regenerator. The working fluid must attain a temperature of T_H before the

subsequent isothermal expansion process; therefore, the Stirling engine's heater must add an additional amount of thermal energy that is proportional to the remaining temperature difference, $T_H - T_{sys,L}^{(1)}$, which is shown as step ④. The amount of energy that the regenerator absorbs and returns is proportional to the temperature difference from the regenerative cooling and heating processes, shown in steps ① and ③ respectively, which is denoted as ΔT_{reg}:

$$\Delta T_{reg} = T_H - T_{sys,H}^{(N)} = T_{sys,L}^{(1)} - T_L \tag{2.22}$$

The effectiveness of the regenerator is the fraction of energy absorbed and returned by the regenerator in comparison to the energy required for the cycle (proportional to $T_H - T_L$), which is expressed as:

$$\epsilon_{reg} = \frac{\Delta T_{reg}}{T_H - T_L} \tag{2.23}$$

The regenerator effectiveness is only a function of the target temperatures T_H or T_L and the system settling temperatures $T_{sys,H}^{(N)}$ or $T_{sys,L}^{(1)}$, so Equation (2.21), which is the hot system settling temperature for a single regenerator after steady operating conditions have been reached, can be substituted in Equation (2.23) to yield the regenerator effectiveness for a single regenerator:

$$\epsilon_{reg} = \frac{\gamma}{2\gamma + 1} \tag{2.24}$$

Similarly, for a regenerator with multiple sub-regenerators, the regenerator effective-

ness for steady operating conditions simplifies to:

$$\epsilon_{reg} = \frac{N\gamma}{(N+1)\,\gamma + N} \tag{2.25}$$

Since Stirling engines operate primarily in steady operating conditions, with only a short warm-up period, the remainder of the analysis will consider the thermal behaviour once steady operating conditions have been reached.

2.4 Stirling engine efficiency model

The Stirling engine efficiency is commonly listed as the Carnot efficiency:

$$\eta_{Carnot} = \eta_{Stirling,ideal} = 1 - \frac{T_L}{T_H} \tag{2.26}$$

however, this efficiency considers ideal regeneration ($\epsilon_{reg} = 1$). The derivations in the previous section revealed that regenerator effectiveness is a function of the regenerator thermal mass ratio and number of sub-regenerators. For non-ideal regeneration, the Stirling engine efficiency must also be a function of the regenerator thermal mass ratio and number of sub-regenerators, and an expression is derived to capture this dependence. The Stirling engine efficiency with non-ideal regeneration is expressed as:

$$\eta_{Stirling} = \frac{Q_{in} - Q_{out}}{Q_{in}} \tag{2.27}$$

where:

$$Q_{in} = m_f R T_H \ln(\lambda) + Q_{non\text{-}reg} \tag{2.28}$$

$$Q_{out} = m_f R T_L \ln(\lambda) + Q_{non\text{-}reg} \tag{2.29}$$

and:

$$\lambda = \frac{V_{max}}{V_{min}} \tag{2.30}$$

An additional $Q_{non\text{-}reg}$ term in Equations (2.28) and (2.29) is required since it represents the amount of supplemental thermal energy that the heater and cooler of the Stirling engine must either add or reject, respectively, to attain target temperatures, T_H and T_L, due to non-ideal regeneration. The regeneration process in the Stirling cycle is isochoric, hence the additional heat added and rejected is:

$$Q_{non\text{-}reg} = (1 - \epsilon_{reg})\, m_f c_{v,f} (T_H - T_L) \tag{2.31}$$

Equation (2.31) is then substituted into Equations (2.28) and (2.29), which are then substituted into Equation (2.27) to generate an expression for the thermal efficiency of the Stirling engine that incorporates the influence of the regenerator effectiveness (Equation (2.25)), as follows:

$$\eta_{Stirling} = \frac{R (T_H - T_L) \ln(\lambda)}{R T_H \ln(\lambda) + (1 - \epsilon_{reg})\, c_{v,f} (T_H - T_L)} \tag{2.32}$$

By substituting Equation (2.25) into Equation (2.32), the following expression is obtained:

$$\eta_{Stirling} = \frac{[(N+1)\gamma + N]\, R\, (T_H - T_L) \ln(\lambda)}{[(N+1)\gamma + N]\, RT_H \ln(\lambda) + (N+\gamma)\, c_{v,f}\, (T_H - T_L)} \tag{2.33}$$

It is shown in Equation (2.33) that the efficiency of the Stirling engine is not only dependent on the target temperatures, T_H and T_L, as seen in Equation (2.26), but is also a function of the compression ratio, λ, the properties of the employed fluid, $c_{v,f}$ and R (specific gas constant), the regenerator thermal mass ratio, γ, and the number of sub-regenerators, N.

Chapter 3

Experimental apparatus

A regenerator test apparatus was designed and built by undergraduate student, Brayden T. York, to validate the heat transfer model developed in Section 2.3. The regenerator test apparatus, which is shown in Figure 3.1, consisted of two linear pneumatic actuators that were programmed to move the hot and cold pistons in an oscillatory manner for a constant volume regeneration process at an equivalent rotational speed of 180 rpm. The apparatus also employed a PID controlled electric heat source, an air-flow regulator to control the motion of the pistons, and a data acquisition module to process the signal generated by the thermocouples. Each sub-regenerator consisted of a 304 stainless steel wire mesh with a wire diameter of approximately 0.04 mm, which are the same specifications that were reported for the GPU-3 Stirling engine [4, 6], and air was used as the working fluid in the experiments. The two regenerator configurations that were examined in the experiments were spaced and unspaced sub-regenerators. The number of sub-regenerators was set at both 12 and 16 sub-regenerators, which corresponds to a regenerator thermal mass ratio of $\gamma =$

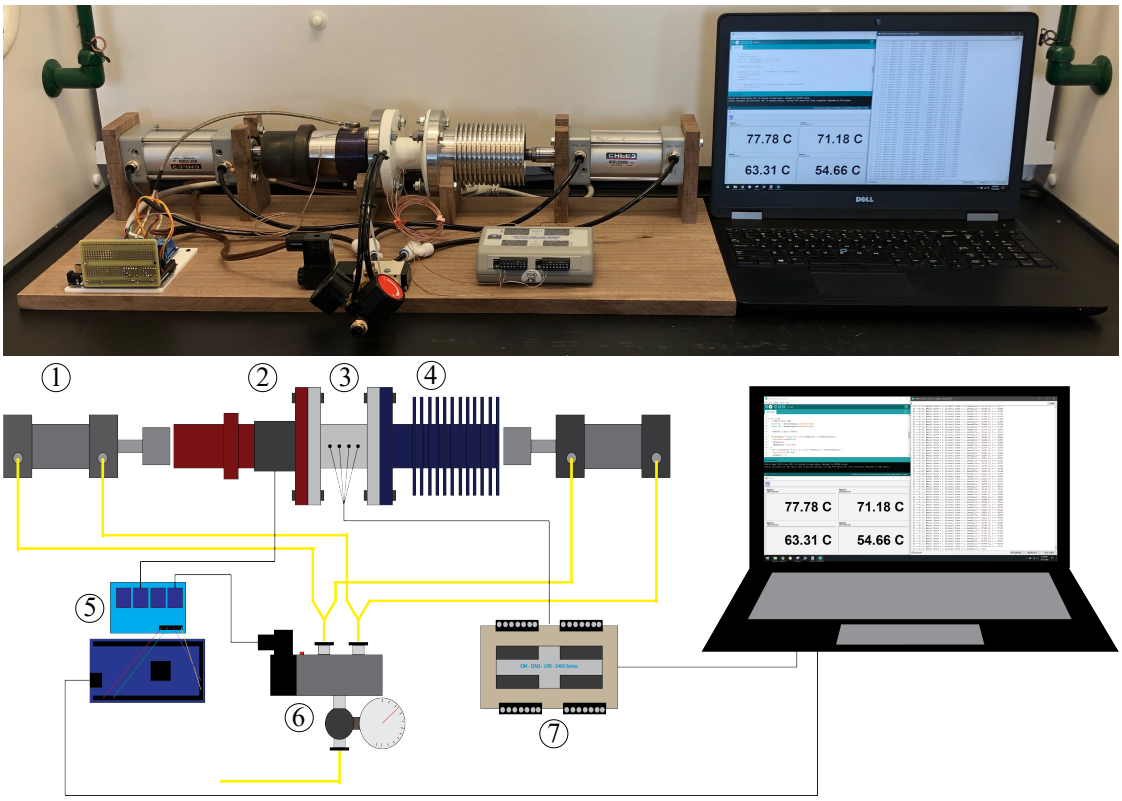

Figure 3.1: Experimental setup of the regenerator test apparatus with **1)** linear pneumatic actuators, **2)** hot cylinder, **3)** regenerator chamber, **4)** cold cylinder, **5)** PID controller, **6)** air-flow regulator, and **7)** data acquisition module.

4.01:1 and $\gamma = 5.35$:1, respectively. An unspaced sub-regenerator configuration denotes that there is physical contact between neighbouring sub-regenerators, while a spaced configuration indicates that each sub-regenerator was separated by a ceramic insulation ring to actively minimize the local axial conduction between each sub-regenerator. Thermocouples were placed at the centre of every group of four sub-regenerators to record the temperature at the 2^{nd}, 6^{th}, 10^{th}, and 14^{th} sub-regenerators. The heat source and heat sink temperatures were measured using thermocouples that recorded the inside air temperatures of both hot and cold cylinders, and their respective temperatures were maintained at approximately $T_H = 353$ K (80°C) and $T_L = 303$ K (30°C) for every test case. Each experiment was run for at least 40 minutes

to ensure that the working fluid and regenerator reached steady operating conditions. The results gathered from the experiments were then compared against those obtained from the heat transfer model to assess its validity.

Chapter 4

Results and discussion

4.1 Single regenerator analysis

A single regenerator is first analyzed to determine the limitations for regenerator effectiveness of a single regenerator setup. The regenerator effectiveness described in Equation (2.24) is only a function of the regenerator thermal mass ratio, and thus is plotted in Figure 4.1 against a range of values for the regenerator thermal mass ratio. It can be seen in Figure 4.1 that the maximum effectiveness a single regenerator can attain is 50%. As the regenerator thermal mass ratio increases, the regenerator effectiveness increases asymptotically towards a maximum value of 50%. This maximum effectiveness of a single regenerator applies to any regenerator composed of a continuous material with high thermal conductivities and small thicknesses, satisfying the conditions from Equations (2.3) and (2.13), such as parallel plates. From this analysis it is demonstrated that single regenerators, such as parallel plate regenerators, with specifications that satisfy the thermal equilibrium approximation, cannot attain

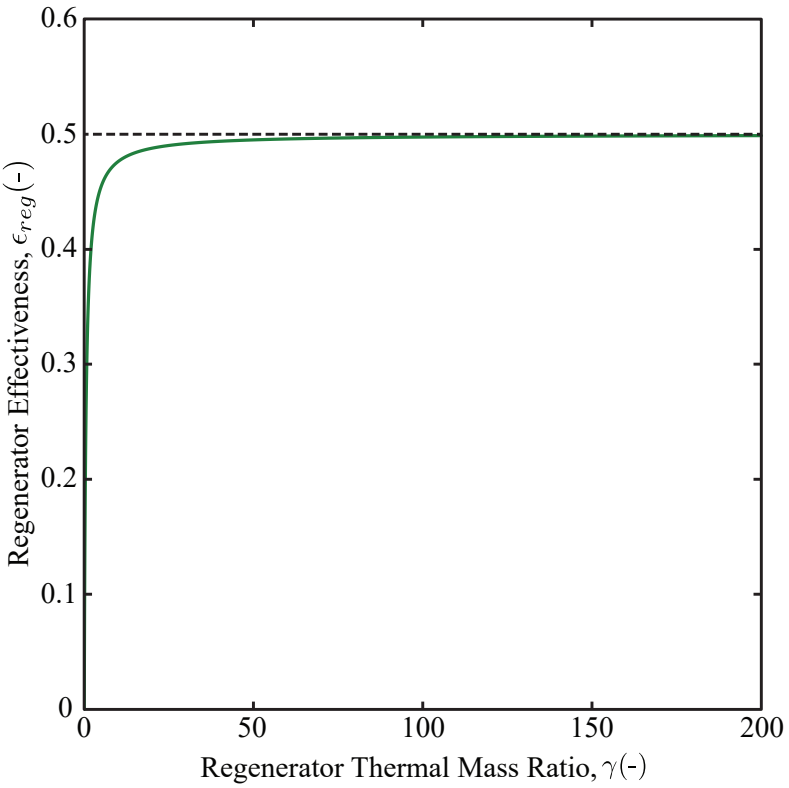

Figure 4.1: Regenerator effectiveness, ϵ_{reg}, of a single regenerator, $N = 1$, as a function of the regenerator thermal mass ratio, γ.

a regenerator effectiveness greater than 50%. The following sections in this study will reveal how to obtain a regenerator effectiveness greater than 50%, and how to design for an effectiveness greater than 95%.

4.2 Multiple sub-regenerator analysis

4.2.1 Influence of number of sub-regenerators

Using Equations (2.16)-(2.19), the temperature distributions of regenerators composed of various numbers of sub-regenerators for a regenerative cooling process were plotted in Figure 4.2. For this analysis the regenerator thermal mass ratio remained constant and the regenerator mass was distributed evenly across the sub-regenerators.

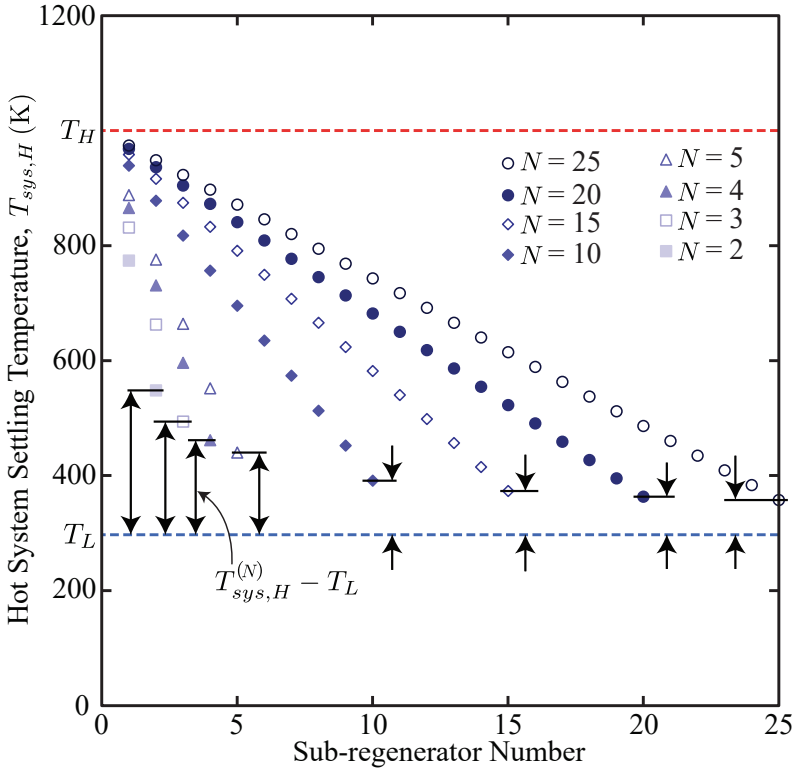

Figure 4.2: Temperature distribution within regenerators with varying number of sub-regenerators, N, and constant regenerator thermal mass ratio, $\gamma = 20{:}1$, during a regenerative cooling process for steady operating conditions.

It is shown that as the number of sub-regenerators increases, the temperature of the last sub-regenerator and correspondingly the exiting working fluid becomes closer to the cold target temperature, T_L. Therefore, the temperature difference between the exiting working fluid and cold target temperature ($T^{(N)}_{sys,H} - T_L$) decreases and regenerator effectiveness increases, according to Equation (2.23). Figure 4.2 also reveals that regenerators composed of multiple sub-regenerators maintain a linear temperature distribution, which is crucial for enhancing the regenerator effectiveness. This linear temperature profile also indicates that average regenerator temperatures should be evaluated using an arithmetic mean between the first and last sub-regenerators, rather than using a log-mean temperature difference, as is often done in the literature. In

summary, increasing the number of sub-regenerators enables the last sub-regenerator and exiting working fluid to achieve a temperature closer to the target temperature, which enhances the regenerator's effectiveness. The influence of the number of sub-regenerators and regenerator thermal mass ratio on the effectiveness of Stirling engine regenerators will now be quantified.

4.2.2 Multiple sub-regenerator effectiveness

The regenerator effectiveness from Equation (2.25) is plotted against the number of sub-regenerators with various thermal mass ratio values in Figure 4.3, which shows that increasing both the regenerator thermal mass ratio and number of sub-regenerators enhances the effectiveness of the regenerator. To determine the maximum attainable effectiveness, an infinite regenerator thermal mass ratio ($\gamma = \infty$:1) can be substituted into Equation (2.25) to yield:

$$\epsilon_{reg,max} = \frac{N}{N+1} \tag{4.1}$$

which represents the maximum effectiveness that a regenerator can attain based on the number of sub-regenerators employed (N), analogous to the Carnot efficiency for heat engines. The maximum effectiveness from Equation (4.1) is plotted in Figure 4.3 to show the upper limitation on the regenerator effectiveness value versus the number of sub-regenerators used.

The ability to achieve a specific value for the regenerator effectiveness based on the number of sub-regenerators (N) and regenerator thermal mass ratio (γ) is pre-

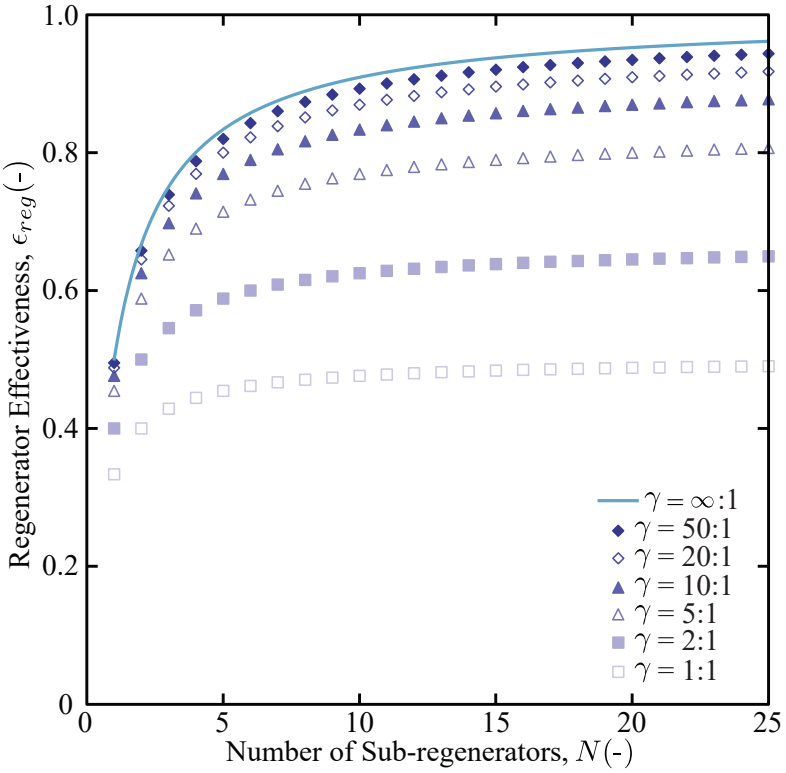

Figure 4.3: Regenerator effectiveness, ϵ_{reg}, as a function of the number of sub-regenerators, N, and regenerator thermal mass ratio, γ, in comparison to the maximum regenerator effectiveness when $\gamma = \infty$:1.

sented and can be used in the design of a Stirling engine regenerator. Figure 4.4 is a plot of Equation (2.25), which shows how to select the values of both the number of sub-regenerators and the regenerator thermal mass ratio to achieve regenerator effectiveness values of 95%, 96%, 97%, and 98%. Any values above and to the right of the effectiveness lines will result in a higher regenerator effectiveness. It is also shown in Figure 4.4 that the effectiveness lines approach a vertical asymptote as the number of sub-regenerators decreases. This occurs since each regenerator effectiveness has a corresponding minimum required number of sub-regenerators to attain the specified effectiveness. For example, to attain 95% regenerator effectiveness, the minimum required number of sub-regenerators is 19, and it is impossible for a regenerator with

less than 19 sub-regenerators to attain 95% effectiveness. It should be noted that the GPU-3 Stirling engine's regenerator, which implemented 308 stacked sub-regenerators and a regenerator thermal mass ratio of 235:1 [4, 6], had an effectiveness of approximately 99.2%, according to Equation (2.25). This value of regenerator effectiveness produces a Stirling engine efficiency of 69.6% when using a compression ratio of 10:1, hydrogen as the working fluid, and target operating temperatures, $T_H = 1000$ K and $T_L = 300$ K, according to (2.33). A value of 80 sub-regenerators and a regenerator thermal mass ratio of 125:1 corresponds to a regenerator effectiveness of 98%, which produces a Stirling engine efficiency of 68.9% with the same compression ratio,

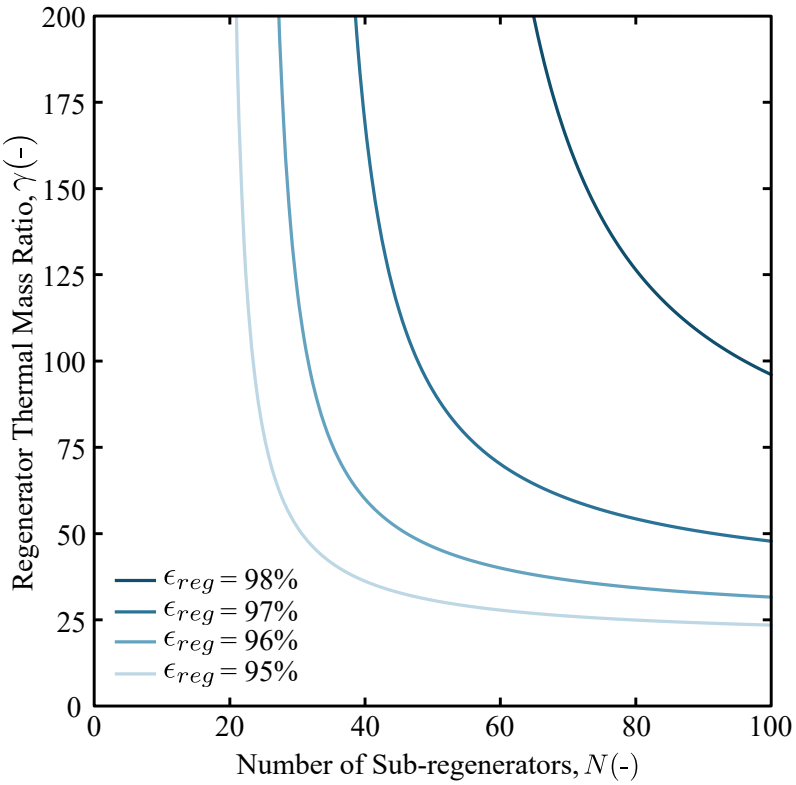

Figure 4.4: Plot of the regenerator effectiveness curves (for 95%, 96%, 97%, and 98%) and the corresponding values of the regenerator thermal mass ratio, γ, and number of sub-regenerators, N, required to produce a desired effectiveness.

working fluid properties, and target operating temperatures. Thus, Stirling engine designers can use Equation (2.25) to select a regenerator effectiveness they desire based on the selected regenerator thermal mass ratio and the number of sub-regenerators employed.

4.2.3 Influence of mass distribution

An interesting question that arises in the design of regenerators is: does the distribution of the sub-regenerator mass influence the regenerator effectiveness? To simulate an uneven mass distribution, the regenerator thermal mass ratio values in Equation (2.16)-(2.19) were varied for each of the sub-regenerators over a wide range of distributions. The analysis revealed that the regenerator effectiveness is a function of the non-uniformity of the mass distribution, which is described by the standard deviation of the regenerator thermal mass ratio, σ, and the arrangement of the distribution did not matter. The regenerator effectiveness is plotted against the standard deviation in Figure 4.5, which shows that as the standard deviation increases, which corresponds to an increasingly uneven distribution of the sub-regenerator mass, the regenerator effectiveness decreases until it reaches the value for a single regenerator (with the corresponding regenerator thermal mass ratio). The reason that the regenerator effectiveness approaches the value for a single regenerator as the standard deviation increases is because an extremely uneven mass distribution approximates that of a single regenerator. It is concluded from this analysis that the optimum sub-regenerator mass distribution for a Stirling engine regenerator is a uniform mass distribution.

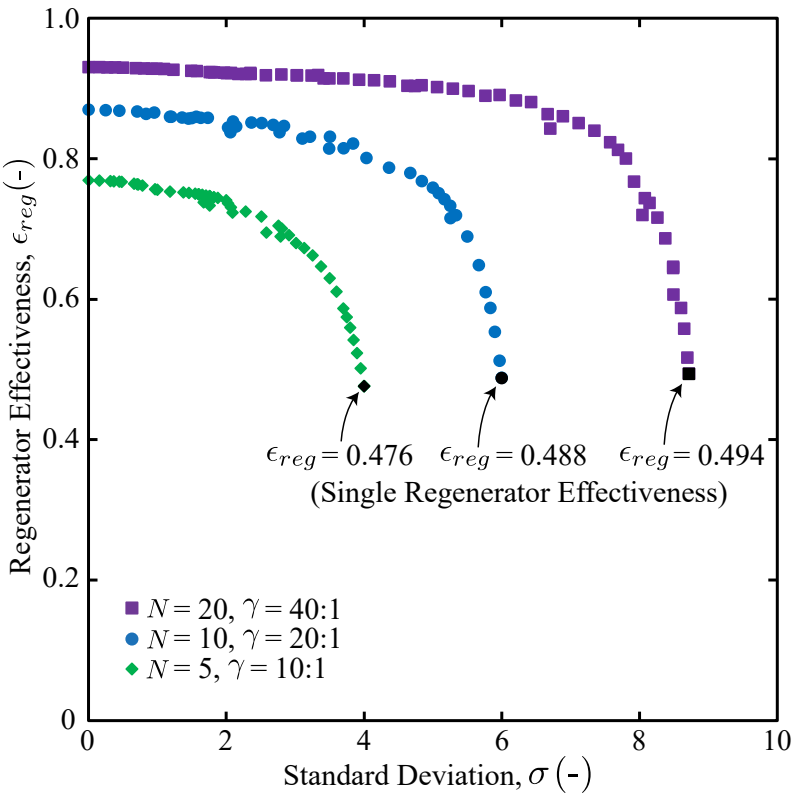

Figure 4.5: Regenerator effectiveness, ϵ_{reg}, as a function of the standard deviation, σ, of the distribution of the regenerator thermal mass ratio among the sub-regenerators for three different cases. The black points indicate the ϵ_{reg} values that coincide with a single regenerator.

4.2.4 Experimental validation

Validation of the heat transfer model is necessary to ascertain that the derived expressions can generate accurate predictions of the thermal behaviour in Stirling engine regenerators. To ensure that the experiments were eligible to be compared against the heat transfer model developed in Section 2.3, the conditions described in Equations (2.3) and (2.13) had to be satisfied. The highest resultant Biot number from the experiments was 6.5×10^{-4}, and the highest regeneration time ratio value, ζ, was 0.82, thus demonstrating that the experiments satisfied the conditions. The experi-

mental and theoretical results of regenerative heating and cooling processes for spaced and unspaced sub-regenerator configurations are shown in Figures 4.6(a) and (b), for 12 and 16 sub-regenerators, respectively. It is shown that there is good agreement between the experimental and theoretical results with percent differences ranging between 0.14% to 2.4% for 12 sub-regenerators (0.47 K to 7.73 K), and 0.01% to 1.96% for 16 sub-regenerators (0.03 K to 6.68 K). The experimental results shown in Figures 4.6(a) and (b) also confirm that the temperature distribution within the regenerator is linear. Since there is good agreement between the heat transfer model and experimental results, it is confirmed that the heat transfer model has been validated and can be used in the design of Stirling engine regenerators to predict their effectiveness based on the selected values of regenerator thermal mass ratio and number of sub-regenerators.

4.2.5 How to thermally isolate sub-regenerators

Another interesting question that arises from the results of this study is: how can a designer ensure that there is sufficient thermal isolation between sub-regenerators to yield a regenerator configuration that has multiple sub-regenerators and is not behaving as a single regenerator? To examine this experiments were performed for two sub-regenerator configurations: spaced and unspaced, where the wire meshes used to form the regenerator were either directly in contact or separated by a ceramic insulation ring, respectively. It is shown in Figures 4.6(a) and (b) that the experimental values of spaced and unspaced configurations are nearly identical, with an average

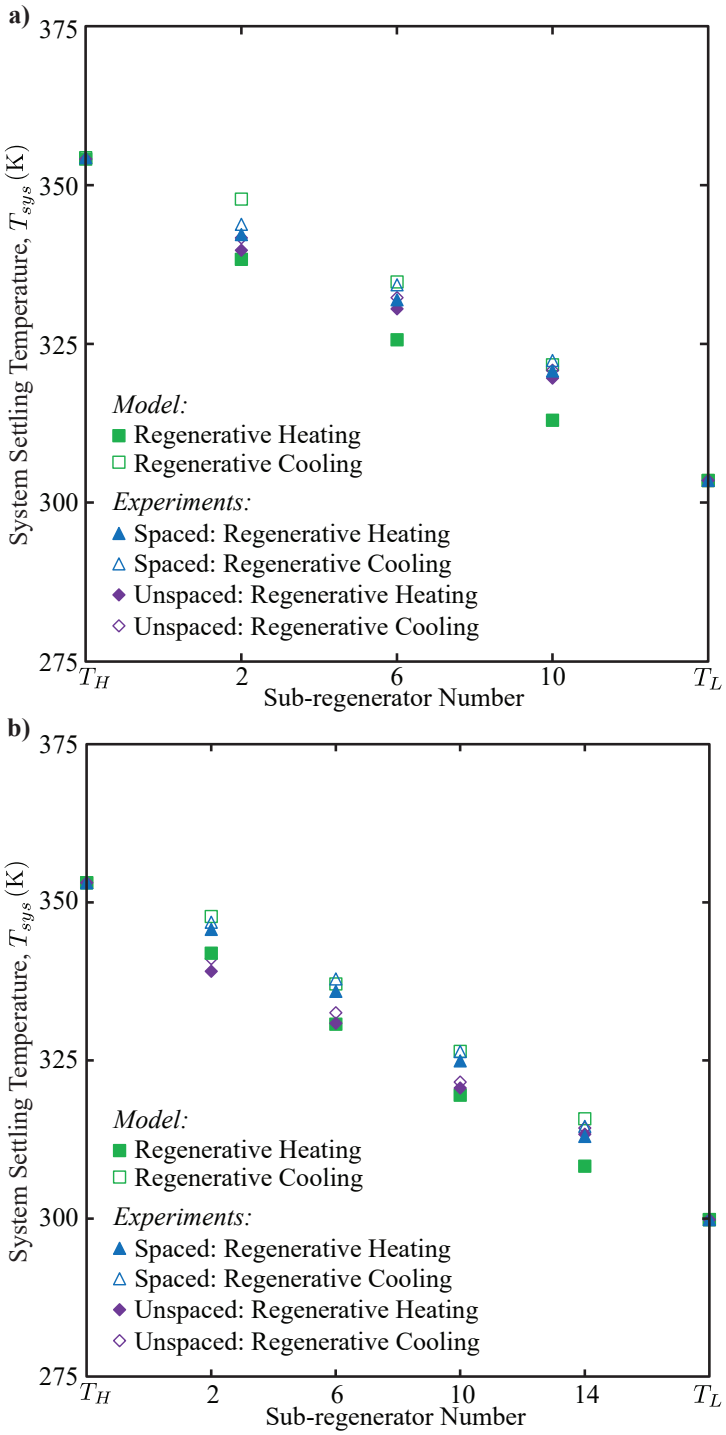

Figure 4.6: Comparison between the results predicted by the heat transfer model and experimental results for spaced and unspaced sub-regenerators for regenerative heating and cooling processes with **a)** $N = 12$ and $\gamma = 4.01{:}1$, and **b)** $N = 16$ and $\gamma = 5.35{:}1$.

percent difference of 0.53% for 12 sub-regenerators (1.78 K), and 1.21% for 16 sub-regenerators (4.06 K). Figures 4.6(a) and (b) reveal that unspaced sub-regenerators, such as wire meshes stacked directly against one another, provide sufficient thermal contact resistance to be considered as thermally isolated. Therefore, Stirling engine designers can simply stack wire mesh sub-regenerators together to attain the required thermal resistance to produce a sufficient temperature distribution, rather than needing to space each individual sub-regenerator or use other complex isolation strategies.

4.3 Stirling engine efficiency

The efficiency of Stirling engines is ultimately the most important outcome when designing regenerators. A parametric analysis using Equation (2.33) was performed to examine the effects of the regenerator thermal mass ratio and number of sub-regenerators on the efficiency of Stirling engines, and to compare the resultant efficiencies with that of the Carnot cycle (ideal regeneration).

4.3.1 Effect of number of sub-regenerators

The number of sub-regenerators directly influences the effectiveness of the regenerator, which subsequently impacts the thermal efficiency of the Stirling engine, as seen in Equation (2.32). In this portion of the parametric analysis, the number of sub-regenerators was varied from 1 to 25 for various target temperature ratios, T_H/T_L, while the compression ratio was fixed at a value of 10:1, the employed working fluid was hydrogen, and the regenerator thermal mass ratio was fixed at a value of 20:1. It

is shown in Figure 4.7(a) that as the number of sub-regenerators increases, Stirling engine efficiency also increases, as expected with an increasing regenerator effectiveness. It is seen, however, that the incremental increase in Stirling engine efficiency decreases as the number of sub-regenerators increase, illustrated by the lines becoming progressively closer together, which indicates that there are diminishing returns as the number of sub-regenerators is increased. Therefore, Figure 4.7(a) can be used by Stirling engine designers to select an appropriate value for the number of sub-regenerators required to achieve a desired value for the Stirling engine efficiency. The selection of an appropriate number of sub-regenerators will avoid the use of an excessive number of sub-regenerators, which could impede the flow of the working fluid through the regenerator and increase the pressure drop.

4.3.2 Effect of regenerator thermal mass ratio

The regenerator thermal mass ratio also influences the effectiveness of the regenerator, which subsequently impacts the thermal efficiency of the Stirling engine, as seen in Equation (2.32). In this portion of the parametric analysis, the value of the regenerator thermal mass ratio was varied from 1:1 to ∞:1 for various target temperature ratios, T_H/T_L, while the compression ratio was fixed at a value of 10:1, the employed working fluid was hydrogen, and the number of sub-regenerators was fixed at a value of 25. It is shown in Figure 4.7(b) that as the value of the regenerator thermal mass ratio increases, the Stirling engine's efficiency also increases, as expected with an increasing regenerator effectiveness. There are also diminishing returns as the re-

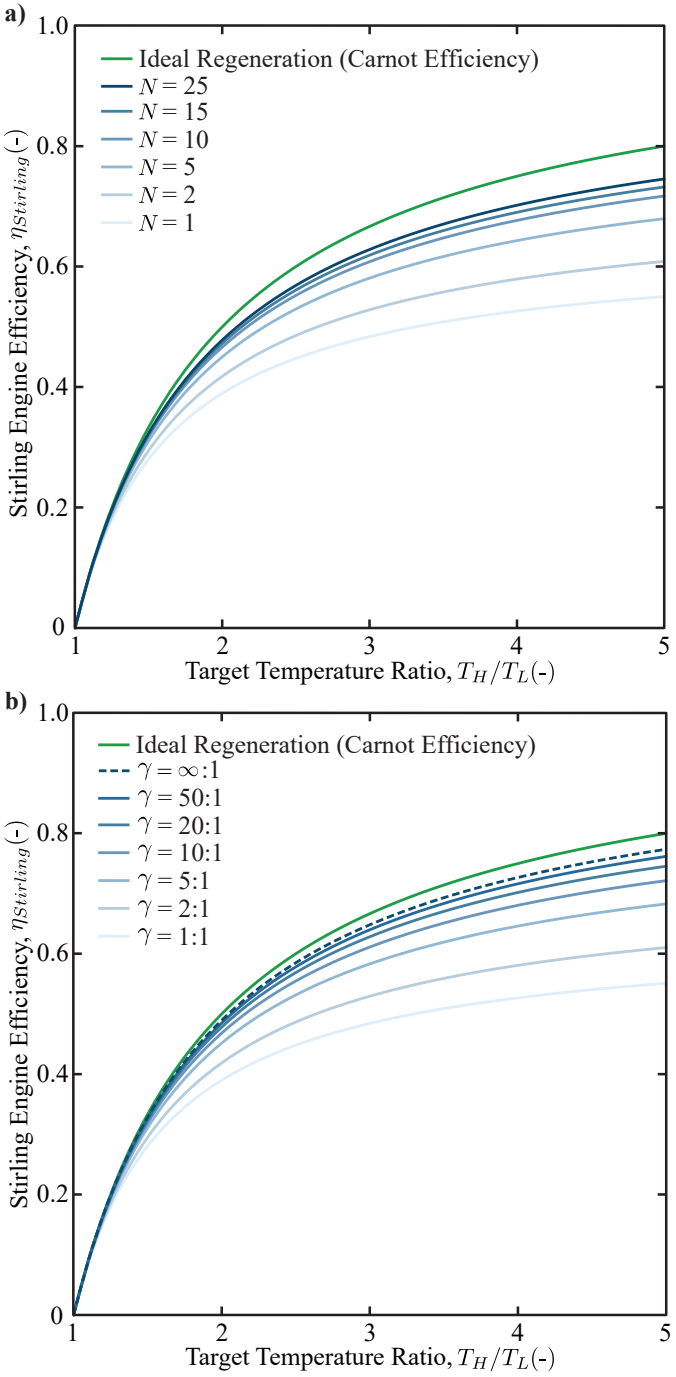

Figure 4.7: Stirling engine efficiency versus target temperature ratio for: **a)** varying number of sub-regenerators, N, with constant compression ratio, λ = 10:1, constant working fluid properties (hydrogen), and constant regenerator thermal mass ratio, γ = 20:1, and **b)** varying regenerator thermal mass ratio, γ, with constant compression ratio, λ = 10:1, constant working fluid properties (hydrogen), and constant number of sub-regenerators, N = 25.

generator thermal mass ratio approaches ∞:1, as illustrated by the lines becoming progressively closer together. Similarly to the number of sub-regenerators, Figure 4.7(b) can be used by Stirling engine designers to select an appropriate value of the regenerator thermal mass ratio required to achieve a desired value for the Stirling engine efficiency. The selection of an appropriate value of the regenerator thermal mass ratio will avoid the use of an unnecessary amount of regenerator mass.

Chapter 5

Conclusions

This chapter summarizes the conclusions of this thesis, provides recommendations for future study, and discusses the important contributions. It starts with a summary of the objectives described in Chapter 1 to reiterate the purpose of this thesis, and to provide context for the conclusions. Again, the objectives of this thesis were to accomplish the following:

- Determine the settling temperature of the regenerator and working fluid for regenerators composed of single and multiple sub-regenerators;
- Determine which parameters have an influence on the effectiveness of regenerators, and which can be neglected;
- Derive expressions for the regenerator effectiveness and Stirling engine efficiency as a function of the important parameters;
- Determine the sub-regenerator mass distribution that corresponds to maximum regenerator effectiveness;

- Experimentally validate the heat transfer model.

5.1 Conclusions

In this thesis, a discrete one-dimensional transient heat transfer model of a single regenerator was developed to determine the thermal response of the regenerator and working fluid, simultaneously. A parametric analysis of the transient model revealed that, for a single regenerator (one sub-regenerator), the only parameter that influences its effectiveness is the regenerator thermal mass ratio, and the remaining parameters (the convective heat transfer coefficient, regenerator material properties, and regenerator wire radius) can be neglected. These findings were then extended to develop a heat transfer model of a regenerator composed of multiple sub-regenerators, and expressions for the regenerator effectiveness were derived to incorporate the influence of the regenerator thermal mass ratio and number of sub-regenerators, as shown in Equations (2.24) and (2.25). It was found that as the regenerator thermal mass ratio increases, the regenerator effectiveness increases up to a limit, which then became purely dependent on the number of sub-regenerators that the regenerator is composed of, which is shown in Equation (4.1). It was also demonstrated that a minimum of 19 sub-regenerators are required to attain a regenerator effectiveness of 95%, and it was revealed that a uniform sub-regenerator mass distribution provides maximum regenerator effectiveness. Experiments using a Stirling engine regenerator test apparatus were then performed, and the obtained results validated the heat transfer model developed in Section 2.3, thus confirming that this model can be used with confidence

in the design of Stirling engine regenerators. These experiments also demonstrated that stacking sub-regenerators, such as wire meshes, provides sufficient thermal resistance to produce a temperature distribution that enhances regenerator effectiveness. It was also revealed that the Stirling engine efficiency is not only a function of the operating temperatures, but also a function of the properties of the employed working fluid, the Stirling engine's compression ratio, the regenerator thermal mass ratio, and the number of sub-regenerators, which is shown in Equation (2.33). As a result of this thesis, Stirling engine designers can select a value for the regenerator thermal mass ratio and number of sub-regenerators to attain a desired effectiveness, and/or a desired value of the Stirling engine efficiency.

5.2 Recommendations

The following points offer recommendations for future research topics that are beyond the scope of this thesis, which aim to further improve the effectiveness of regenerators, and the performance and efficiency of Stirling engines:

- It is suggested that a study is performed to investigate the pressure drop through the regenerator to determine its functional dependence on the number of sub-regenerators, the diameter of the regenerator wire, the gap size between wires, and the length of the regenerator channel. Experiments should be conducted initially to quantify the pressure drop as a function of the aforementioned parameters, and numerical simulations should follow in attempt to match the experimental results;

- With the results obtained in this thesis and the hypothetical results from the previous recommendation, an optimization analysis could be performed to determine the optimum number of sub-regenerators to complete the necessary heat exchange while limiting the resultant pressure drop for a given regenerator thermal mass ratio. This study would enable Stirling engine designers to select an optimum value for the number of sub-regenerators to enhance regenerator effectiveness and improve Stirling engine performance and efficiency. The findings from this study should then be implemented in an actual Stirling engine to examine its performance and efficiency with various numbers of sub-regenerators and regenerator thermal mass ratios to validate the theoretical results;

- Past studies have shown interest in continuous regenerators with a high thermal conductivity and small material thickness due to their favorable flow characteristics. However, it was shown in this thesis that regenerators of this nature are limited to a maximum effectiveness of 50%. If the thermal conductivity of the regenerator is decreased, though, this could enable continuous regenerators to sustain a sufficient temperature distribution while still reducing the resultant pressure drop of the working fluid and attain an effectiveness greater than 50%. A study should be undertaken to investigate the required thermal conductivity a continuous regenerator must possess to produce a temperature distribution that is comparable to that of thermally isolated sub-regenerators;

- Based on society's overwhelming dependence on fossil fuels, it is understood that the transition from fossil fuel based systems to entirely renewable energy

systems will be strenuous, and will perhaps take several decades. Furthermore, the planet's rapidly depleting and finite reserves of fossil fuel will provide society with no choice but to eventually become reliant on alternative fuel sources. Thus, it is important to develop and invest in transitional and renewable energy technologies, such as Stirling engines, that have the ability to generate power from both fossil fuels and clean energy sources in order to ease this progression;

- Currently, Stirling engines are a relatively unknown technology that can alleviate the global demand for clean energy due to their versatility and ability to attain high efficiencies. This study shows that there is great potential for future advancements in Stirling engine technologies, and reveals that there are more opportunities for impactful discoveries that could enhance the performance and feasibility of Stirling engines.

5.3 Contributions

My contributions to the field involve an enhanced understanding of regenerator design, particularly the design of regenerators to attain a specific Stirling engine efficiency. Prior to my work, designing a regenerator to achieve a certain effectiveness and the limitations associated with single regenerators were not well understood. This thesis is of particular importance since it reveals that only the number of sub-regenerators and regenerator thermal mass ratio influence the effectiveness of Stirling engine regenerators, and outlines the values of each

that correspond to a desired regenerator effectiveness. This is the first study to show that a minimum of 19 sub-regenerators are required to attain 95% regenerator effectiveness, and a uniform sub-regenerator mass distribution maximizes regenerator effectiveness. Stirling engine designers can use this thesis to develop regenerators that enhance Stirling engine efficiency.

Bibliography

[1] D. Sinton. Energy: the microfluidic frontier. *Lab on a Chip*, 14(17):3127–3134, 2014.

[2] K. Emanuel. Increasing destructiveness of tropical cyclones over the past 30 years. *Nature*, 436(7051):686, 2005.

[3] S. Fink. Hurrican katrina: after the flood, 2014.

[4] W. R. Martini. *Stirling engine design manual, 2nd edition*. US Department of Energy, Conservation and Renewable Energy, Office of Vehicle and Engine R&D, 1983.

[5] S. Ranieri, G. Prado, and B. MacDonald. Efficiency reduction in stirling engines resulting from sinusoidal motion. *Energies*, 11(11):2887, 2018.

[6] W. R. Martini. *Stirling engine design manual*. US Department of Energy, Office of Conservation and Solar Applications, Division of Transportation Energy Conservation, 1978.

[7] M. Tanaka, I. Yamashita, and F. Chisaka. Flow and heat transfer characteristics of the Stirling engine regenerator in an oscillating flow. *JSME Int J. II-Fluid*, 33(2):283–289, 1990.

[8] S. Isshiki, A. Sakano, I. Ushiyama, and N. Isshiki. Studies on flow resistance and heat transfer of regenerator wire meshes of Stirling engine in oscillatory flow. *JSME Int J B-Fluid T*, 40(2):281–289, 1997.

[9] J. Sodre and J. Parise. Friction factor determination for flow through finite wire-mesh woven-screen matrices. *J Fluids Eng*, 119(4):847–851, 1997.

[10] I. Yamashita and K. Hamaguchi. Effect of entrance and exit areas on the pressure drop and velocity distribution in regenerator matrix. *JSME Int J B-Fluid T*, 42(3):498–505, 1999.

[11] Z. Yu, X. Mao, and A. J. Jaworski. Experimental study of heat transfer in oscillatory gas flow inside a parallel-plate channel with imposed axial temperature gradient. *Int J Heat Mass Trans*, 77:1023–1032, 2014.

[12] S. C. Costa, M. Tutar, I. Barreno, J. A. Esnaola, H. Barrutia, D. García, M. A. González, and J. I. Prieto. Experimental and numerical flow investigation of Stirling engine regenerator. *Energy*, 72:800–812, 2014.

[13] G. Xiao, H. Peng, H. Fan, U. Sultan, and M. Ni. Characteristics of steady and oscillating flows through regenerator. *Int J Heat Mass Trans*, 108:309–321, 2017.

[14] M. Ni, H. Peng, U. Sultan, K. Luo, and G. Xiao. A quantitative method to describe the flow characteristics of an oscillating flow including porous media. *Int J Heat Mass Trans*, 119:860–866, 2018.

[15] S. Costa, I. Barreno, M. Tutar, J. Esnaola, and H. Barrutia. The thermal non-equilibrium porous media modelling for CFD study of woven wire matrix of a Stirling regenerator. *Energy Convers Manag*, 89:473–483, 2015.

[16] S. Costa, H. Barrutia, J. A. Esnaola, and M. Tutar. Numerical study of the pressure drop phenomena in wound woven wire matrix of a Stirling regenerator. *Energy Convers Manag*, 67:57–65, 2013.

[17] S. Costa, H. Barrutia, J. A. Esnaola, and M. Tutar. Numerical study of the heat transfer in wound woven wire matrix of a Stirling regenerator. *Energy Convers Manag*, 79:255–264, 2014.

[18] I. Barreno, S. Costa, M. Cordon, M. Tutar, I. Urrutibeascoa, X. Gomez, and G. Castillo. Numerical correlation for the pressure drop in Stirling engine heat exchangers. *Int J Therm Sci*, 97:68–81, 2015.

[19] T. Zhao and P. Cheng. Experimental studies on the onset of turbulence and frictional losses in an oscillatory turbulent pipe flow. *Int J Heat Fluid Flow*, 17(4):356–362, 1996.

[20] S. Alfarawi, R. Al Dadah, and S. Mahmoud. Potentiality of new miniature-channels Stirling regenerator. *Energy Convers Manag*, 133:264–274, 2017.

[21] S. Alfarawi, R. Al Dadah, and S. Mahmoud. Transient investigation of mini-channel regenerative heat exchangers: Combined experimental and CFD approach. *Appl Therm Eng*, 125:346–358, 2017.

[22] Z. Li, Y. Haramura, Y. Kato, and D. Tang. Analysis of a high performance model Stirling engine with compact porous-sheets heat exchangers. *Energy*, 64:31–43, 2014.

[23] Z. Li, Y. Haramura, D. Tang, and C. Guo. Analysis on the heat transfer characteristics of a micro-channel type porous-sheets Stirling regenerator. *Int J Therm Sci*, 94:37–49, 2015.

[24] R. Tew, M. Ibrahim, D. Danila, T. Simon, S. Mantell, L. Sun, D. Gedeon, K. Kelly, J. McLean, J. Wood, et al. A microfabricated involute-foil regenerator for Stirling engines. In *5th Intl Energy Convers Eng Conf and Exhib (IECEC)*, page 4739, 2007.

[25] R. F. Costa and B. D. MacDonald. Comparison of the net work output between Stirling and Ericsson cycles. *Energies*, 11(3):670, 2018.

[26] D. A. Blank, G. W. Davis, and C. Wu. Power optimization of an endoreversible stirling cycle with regeneration. *Energy*, 19(1):125–133, 1994.

[27] M. H. Ahmadi, A. H. Mohammadi, and S. Dehghani. Evaluation of the maximized power of a regenerative endoreversible Stirling cycle using the thermodynamic analysis. *Energy Convers Manag*, 76:561–570, 2013.

[28] D. G. Thombare and S. V. Karmare. Theoretical and experimental investigation of α-type bio mass Stirling engine with effect of regenerator effectiveness, heat transfer, and properties of working fluid. *J Renew Sustain Ener*, 4(4):043126, 2012.

[29] B. Kongtragool and S. Wongwises. Thermodynamic analysis of a Stirling engine including dead volumes of hot space, cold space and regenerator. *Renew Energy*, 31(3):345–359, 2006.

[30] S. Kaushik and S. Kumar. Finite time thermodynamic analysis of endoreversible Stirling heat engine with regenerative losses. *Energy*, 25(10):989–1003, 2000.

[31] R. Gheith, F. Aloui, and S. B. Nasrallah. Study of the regenerator constituting material influence on a γ-type Stirling engine. *J Mech Sci Technol*, 26(4):1251–1255, 2012.

[32] R. Gheith, F. Aloui, and S. B. Nasrallah. Determination of adequate regenerator for a γ-type Stirling engine. *Appl Energ*, 139:272–280, 2015.

[33] W. L. Chen, K. L. Wong, and H. E. Chen. An experimental study on the performance of the moving regenerator for a γ-type twin power piston Stirling engine. *Energy Convers Manag*, 77:118–128, 2014.

[34] H. Takizawa, N. Kagawa, A. Matsuguchi, and S. Tsuruno. Performance of new matrix for Stirling engine regenerator. In *Energy Conversion Engineering Conference, 2002. IECEC'02. 2002 37th Intersociety*, pages 491–496. IEEE, 2004.

[35] A. S. Abduljalil, Z. Yu, and A. J. Jaworski. Selection and experimental evaluation of low-cost porous materials for regenerator applications in thermoacoustic engines. *Materials & Design*, 32(1):217–228, 2011.

[36] H. Klein and G. Eigenberger. Approximate solutions for metallic regenerative heat exchangers. *Int J Heat Mass Trans*, 44(18):3553–3563, 2001.

[37] A. J. Organ. The wire mesh regenerator of the stirling cycle machine. *Int J Heat Mass Trans*, 37(16):2525–2534, 1994.

[38] F. de Monte and P. Rosa. Linear analysis of rapidly switched heat regenerators in counterflow. *Int J Heat Mass Trans*, 51(13-14):3642–3655, 2008.

[39] P. V. Trevizoli and J. R. Barbosa Jr. Entropy generation minimization analysis of oscillating-flow regenerators. *Int J Heat Mass Trans*, 87:347–358, 2015.

[40] W. L. Chen, K. L. Wong, and Y. F. Chang. A numerical study on the effects of moving regenerator to the performance of a β-type Stirling engine. *Int J Heat Mass Trans*, 83:499–508, 2015.

[41] J. Jones. Performance of a Stirling engine regenerator having finite mass. *J Eng Gas Turb Power*, 108(4):669–673, 1986.

[42] D. Dai, F. Yuan, R. Long, Z. Liu, and W. Liu. Imperfect regeneration analysis of Stirling engine caused by temperature differences in regenerator. *Energy Convers Manag*, 158:60–69, 2018.

[43] T. L. Bergman, F. P. Incropera, D. P. DeWitt, and A. S. Lavine. *Fundamentals of Heat and Mass Transfer*. John Wiley & Sons, 2011.

[44] A. Žukauskas. Heat transfer from tubes in crossflow. In *Advances in heat transfer*, volume 8, pages 93–160. Elsevier, 1972.